

POLITECNICO DI MILANO

Facoltà di Ingegneria dei Sistemi

Corso di Laurea Magistrale in Ingegneria Biomedica

Dipartimento di Bioingegneria



CIRCADIAN VARIATIONS IN THE HIPPOCAMPUS OF EPILEPTIC RATS

Relatore Politecnico di Milano: Prof.ssa Anna Maria Bianchi
Co-relatore University of Florida : Dott.Paul R. Carney

Tesi di Laurea di :
Stefano Re Fraschini
matr.764277

Anno Accademico 2011- 2012

To my parents, who supported me morally and economically during all my years of
studying

ACKNOWLEDGMENTS

A conclusione di questo mio percorso di studi, intendo ringraziare i professori e collaboratori del Dipartimento di Bioingegneria del Politecnico di Milano che ho incontrato nel mio percorso universitario e a cui devo anche la realizzazione del mio sogno americano, attraverso il Progetto di doppia Laurea Atlantis CRISP.

Un ringraziamento particolare ai Professori Giuseppe Baselli e Alberto Redaelli, che, supportandomi con preziosi consigli e suggerimenti, hanno seguito i miei progressi presso l'University of Florida durante la mia permanenza oltreoceano, e Anna Maria Bianchi relatrice per il Politecnico di questa mia tesi.

Un sentito ringraziamento anche ai miei compagni di avventura in America, Daniele che mi ha ospitato a Houston e accompagnato alla scoperta del Texas, e Celine e Alessio, con i quali ho condiviso non solo un anno di studi ma anche di vita. Infine un ringraziamento speciale ai miei familiari e amici che non mi hanno mai fatto mancare il loro sostegno.

I would like to thank all the people who made it possible for me to carry out this research. First of all, Dr. Carney, who allowed me to work in his lab and provided me with the resources that I needed for my work. A special mention goes to David Stanley, who gave me precious help that facilitated my job. I also want to express my appreciation for all my lab mates, who made my experience at the Epilepsy Research Lab a pleasant one.

I would like to acknowledge the Atlantis CRISP program, which provided me the funding and the opportunity to work at University of Florida. None of this would have been possible without it.

TABLE OF CONTENTS

	<u>page</u>
ACKNOWLEDGMENTS.....	3
LIST OF TABLES.....	6
LIST OF FIGURES.....	7
LIST OF ABBREVIATIONS.....	10
INTRODUCTION.....	19
Epilepsy	19
Circadian Rhythms	21
Temporal Lobe Epilepsy	22
Hippocampus.....	24
Anatomy	25
Functions.....	26
EEG Rhythms.....	27
CA1 Region.....	28
Research Goal.....	29
Thesis Overview	29
EXPERIMENTAL DESIGN.....	30
Animal Model.....	30
Protocol Followed	30
Surgery and Electrode Implantation	31
Electrical Stimulation	33
Data Acquisition	33
High Resolution MRI	34
DATA ANALYSIS.....	35
Extraction of the Spectra.....	35
De-trending	38
Averaging.....	40
Sinusoidal Fitting	42
Relative Power.....	43
Total Power.....	44
RESULTS.....	45
Peak Times of the Different Frequency Bands	45
Relative Power.....	49

Daily Variations	49
Relative Variations in Relative Power.....	57
Total Power.....	62
CONCLUSIONS.....	65
FUTURE DEVELOPMENTS	67
LIST OF REFERENCES	68

LIST OF TABLES

<u>Table</u>	<u>page</u>
4-1 Peak times pre-injury for all the bands for all the rats and average values.....	47
4-2 Peak times post-injury for all the bands for all the rats and average values	47
4-3 Difference in the peak times for all the bands for all the rats and average values.	48
4-4 Number of daily variations higher than 10% for all the bands of all the rats and average values, pre-injury	55
4-5 Number of daily variations higher than 10% for all the bands of all the rats and average values, post-injury	55
4-6 Difference in the daily variations higher than 10% for all the bands of all the rats and average values	55
4-7 Number of daily variations higher than 25% for all the bands of all the rats and average values, pre-injury	55
4-8 Number of daily variations higher than 25% for all the bands of all the rats and average values, post-injury	56
4-9 Difference in the daily variations higher than 25% for all the bands of all the rats and average values	56
4-10 Number of variations higher than 10% for all the bands for all the rats and average	61
4-11 Distribution pattern of the variations presented in Table 10.....	61
4-12 Number of variations higher than 25% for all the bands for all the rats and average	61
4-13 Distribution pattern of the variations presented in Table 12.....	61
4-14 Peak times of the total spectral power for all the rats and average, pre-injury ...	63
4-15 Peak times of the total spectral power for all the rats and average, post-injury ..	64

LIST OF FIGURES

<u>Figure</u>	<u>page</u>
1-1 Depiction of the limbic system and its position in the brain.....	24
1-2 Laszlo Seress' preparation of a human hippocampus alongside a sea horse. ...	25
2-1 Placement of the two 16 microwire electrode arrays and of the stimulating electrode.....	32
3-1 The shape of a Hamming window and of its transform.....	37
3-2 Example of plot of the hourly spectral values for the four bands considered.....	38
3-3 Example of a signal composed by the sum of a straight-line and a sinusoid.....	39
3-4 Example of the sinusoid obtained from the de-trending of the signal shown in Figure 3-3, using the technique described above.	39
3-5 Example of de-trended data from this study.	40
3-6 Example of de-trended 24 hour long data	40
3-7 24 hour long segment following the one showed in Figure 3-6.....	41
3-8 Average of the two 24 hour long de-trended segments showed in Figures 3-6 and 3-7	41
3-9 Example of the superposition of the fitting sinusoid to the experimental data	42
4-1 Comparison of the circadian modulation for the four different frequency bands before injury (red) and in the chronic phase (blue)	45
4-2 Comparison of the circadian modulation for the four different frequency bands before injury (red) and in the chronic phase (blue)	46
4-3 Comparison of the circadian modulation for the four different frequency bands before injury (red) and in the chronic phase (blue)	47
4-4 Column graph representing the peak time for each band pre injury and post injury.....	48
4-5 Distribution during the day of the variations in the relative power pre-injury.....	49
4-6 Same as Figure 4-5, but after injury	49
4-7 Distribution during the day of the variations in the relative power pre-injury.....	50

4-8	Same as Figure 4-7, but after injury	50
4-9	Distribution during the day of the variations in the relative power pre-injury.....	51
4-10	Same as Figure 4-9, but after injury	51
4-11	Distribution during the day of the variations in the relative power pre-injury.....	52
4-12	Same as Figure 4-11, but after injury.	52
4-13	Distribution during the day of the variations in the relative power pre-injury.....	53
4-14	Same as Figure 4-13, but after injury	53
4-15	Distribution during the day of the variations in the relative power pre-injury.....	54
4-16	Same as Figure 4-15, but after injury.	54
4-17	Column graph representing the number of variations >10% for each band pre injury and post injury.....	56
4-18	Column graph representing the number of variations >25% for each band pre injury and post injury.....	57
4-19	Distribution of the variations higher than 10%; in red increases, in blue decreases.....	58
4-20	Distribution of the variations higher than 25%; in red increases, in blue decreases.....	58
4-21	Distribution of the variations higher than 10%; in red increases, in blue decreases.....	59
4-22	Distribution of the variations higher than 25%; in blue decreases.	59
4-23	Distribution of the variations higher than 10%; in red increases, in blue decreases.....	60
4-24	Distribution of the variations higher than 25%; in red increases.	60
4-25	Circadian modulation of the total power for rat #1; in red pre-injury, in blue post-injury.....	62
4-26	Circadian modulation of the total power for rat #2; in red pre-injury, in blue post-injury.....	62
4-27	Circadian modulation of the total power for rat #3; in red pre-injury, in blue post-injury.....	63

4-28 Column graph representing the peak time for the total power pre injury and post injury. 64

LIST OF ABBREVIATIONS

DFT	Discrete Fourier Transform
EEG	Electroencephalography
EKG	Electrocardiography
fMRI	Functional Magnetic Resonance Imaging
ILAE	International League Against Epilepsy
MRI	Magnetic Resonance Imaging
PET	Positron Emission Tomography
SCN	Suprachiasmatic Nucleus
TLE	Temporal Lobe Epilepsy

ABSTRACT

Epilepsy is the most common primary disorder of the brain, and, according to the World Health Organization, is one of the leading causes of neuropsychiatric disability worldwide, along with depression. Since the late 19th century it has been observed that epileptic seizures tend to occur at specific times of day, thus suggesting a link between circadian rhythms and epilepsy. However, a thorough understanding of such relationship and its extent is still lacking. This thesis engages in investigating the circadian variations, in terms of frequency rhythms in the EEG signal, in the hippocampus of epileptic rats, during a seizure-free period in the chronic phase of the disease.

The epileptogenic process, which originates from a cerebral lesion, is divided in two phases: latent and chronic. During the latent phase epileptic symptoms are not observable; this phase ends when the first spontaneous epileptic seizure occurs, marking the beginning of the chronic phase, where epileptic symptoms are visible.

Several biologic processes display an approximately 24 hours rhythmicity, which is called circadian (from the latin *circa dies*, “almost a day”). These endogenous rhythms are due to the presence of a biologic clock, the circadian pacemaker, whose principal component is the Supra-Chiasmatic Nucleus, which is responsible of the entraining of the endogenous clock employing environmental cues (*zeitgebers*), among which light is the most relevant. Gowers was the first to record that epileptic seizures tend to occur at specific moments of the day, such as in the morning at arousal or in the night during sleep [1].

Recent studies carried out in Dr. Carney's Epilepsy Research Lab (at the University of Florida) have shown a phase-shift in the circadian modulation of EEG features in the CA1 region in an animal model of TLE, during the latent period of the disease [31, 32, 33]. This study, extending from there, aims at investigating the presence of a similar phase-shift during the chronic phase of the disease.

In-vivo intra-hippocampal recordings were performed on rats, employing 32 microwire electrodes. Following one week of baseline EEG recordings, the animals underwent continuous electrical stimulation, with the purpose of inducing brain injury leading to spontaneous seizures. The animals were kept in a controlled environment with symmetric day/night cycles (lights on at 6 am, lights off at 6 pm) and continuously monitored with a video recording.

Spectral analyses was carried out on these recordings, considering the frequency range 0-100 Hz, which includes all the most relevant hippocampal EEG rhythms (theta: 3-11 Hz, beta: 12-29 Hz, gamma 30-70 Hz, high gamma 71-100 Hz). The circadian modulation of the spectral power of these bands was considered and comparisons were drawn between the pre-injury period and the seizure-free period in the chronic phase of the disease.

To estimate the spectra, the discrete Fourier transform (DFT) with a Hamming window was applied to chunks of signal of duration of 10 seconds, in order to handle the non-stationarity of the EEG signal over longer periods. The spectra estimated in this way were then averaged over an hour, yielding the hourly average spectral power for each of the bands considered; this was done over 4-6 days' worth of data both before stimulation and in the chronic phase.

To underline the circadian modulation, the data, consisting of the series of the hourly spectral power averages, was de-trended and the 24 hours cycle were averaged over a few days and then fitted with a sinusoid. This was done in order to find during which part of the day the peak values for each band were reached, comparing the results before the stimulation and in the chronic phase.

Finally the relative variation in the spectral power of the single band with respect to the total spectral power and of the single band before the stimulation with respect with the chronic phase was taken into account.

At the end of this study a phase-shift in the circadian modulation of the beta rhythm was observed. This confirmed that the phase-shift observed in the latent period is not a transitory phenomenon, but is still present in the chronic phase of the disease, leading to new and interesting hypothesis that will be later discussed in this thesis.

The organization of the thesis is the following:

- Introduction: the chapter introduces the basic concepts to understand the development and aim of the thesis; in particular, the essential information about epilepsy (both in general and on temporal lobe epilepsy), circadian rhythms and the hippocampus (with a particular focus on the CA1 region and the principal EEG rhythms with their relevance) is given.

- Experimental Design: the chapter describes the protocol followed and the experimental set-up, focusing on the principal aspects of the animal model employed.
- Data Analysis: the chapter describes the methodologies employed for the analysis of the experimental data.
- Results: in this chapter the results of the study are presented.
- Conclusions: in the chapter the results presented before are commented and some hypotheses are presented.
- Future developments: finally, in this chapter, possible future studies with the capability of adding new information and verifying the hypotheses presented before are presented.

SOMMARIO

L'epilessia e' il piu' diffuso disordine primario del cervello ed una delle principali cause di disabilita' neuropsichiatrica, insieme alla depressione, secondo l'Organizzazione Mondiale della Sanita'. Sin dalla fine del diciannovesimo secolo e' stato osservato che le crisi epilettiche tendono a presentarsi in precisi momenti della giornata, suggerendo un possibile legame fra epilessia e ritmi circadiani. Tuttavia una spiegazione esaustiva del fenomeno e delle sue possibili implicazioni non e' ancora stata raggiunta. Questa tesi analizza le variazioni circadiane, in termini di ritmi di frequenze nel segnale EEG, nell'ippocampo di ratti epilettici, durante un periodo in cui non si sono presentate crisi, nella fase cronica della malattia.

Il processo di epileptogenesi, originato da una lesione cerebrale, si suddivide in due fasi: latente e cronica. Durante la fase latente non sono osservabili i sintomi dell'epilessia; tale fase si considera terminata quando insorge il primo attacco epilettico spontaneo, che marca l'ingresso nella fase cronica, in cui i sintomi della malattia sono osservabili.

Svariati processi biologici presentano una ritmicita', del periodo di circa 24 ore, che viene percio' definita circadiana (dal latino *circa dies*, "circa un giorno"). La presenza di questi ritmi endogeni e' dovuta alla presenza di un orologio biologico, il pacemaker circadiano, il cui componente principale e' ritenuto essere il Nucleo Supra-Chiasmatico, che e' anche responsabile dell'aggiustamento del clock endogeno e sfrutta alcuni fattori ambientali (*zeitgebers*), fra i quali la luce risulta il piu' rilevante. Gowers fu il primo a registrare come gli attacchi epilettici si verificassero in precisi

momenti della giornata, quali il mattino in prossimità del risveglio o la notte durante il sonno [1].

Studi recenti [31, 32, 33] nel Laboratorio di Ricerca sull'Epilessia del Dott. Paul Carney (presso University of Florida), hanno evidenziato come sia osservabile uno sfasamento nella modulazione circadiana dell'attività neurale nella regione CA1 dell'ippocampo di ratti epilettici durante la fase latente della malattia. Lo scopo di questa tesi è di espandere i risultati precedentemente ottenuti, investigando la fase cronica, per verificare se questo sfasamento fosse ancora presente.

Pertanto sono stati registrati *in-vivo* i segnali elettroencefalografici provenienti dall'ippocampo di alcuni ratti, usando un array di 32 micro-elettrodi. Dopo aver acquisito un'intera settimana di tracciati EEG continui sui ratti sani, questi sono stati sottoposti a stimolazione elettrica al fine di indurre una lesione cerebrale che avrebbe portato allo sviluppo dell'epilessia del lobo temporale. Gli animali sono stati mantenuti in un ambiente controllato con cicli giorno/notte simmetrici (luci accese dalle 6 alle 18) per tutta la durata dello studio, durante il quale sono anche stati continuamente monitorati con registrazioni video, oltre che EEG.

È stata poi applicata un'analisi spettrale sui tracciati EEG così ottenuti, considerando un range di frequenze da 0-100 Hz, nel quale sono racchiusi tutti i principali ritmi elettroencefalografici dell'ippocampo (theta: 3-11 Hz, beta: 12-29 Hz, gamma 30-70 Hz, high gamma 71-100 Hz). È stata presa in considerazione la modulazione circadiana della distribuzione della potenza spettrale fra le diverse bande e sono stati paragonati i dati relativi al periodo precedente alla lesione e a quello successivo alla prima crisi spontanea.

Per la stima degli spettri si è fatto ricorso alla trasformata di Fourier discreta (DFT) su spezzoni di segnali della durata di 10 secondi, per ovviare alla non stazionarietà del segnale EEG su periodi più lunghi, dopo aver applicato una finestra di Hamming. Gli spettri così ottenuti sono stati poi mediati su un arco di un'ora, ottenendo il valore medio orario della potenza spettrale di ognuna delle bande considerate; ciò è stato eseguito su una mole di dati pari a 4-6 giorni di registrazioni continue sia prima della stimolazione che nella fase cronica.

Per evidenziare la modulazione circadiana, si è prima eseguita una operazione di de-trending, per eliminare la deriva della linea di base, poi i cicli di 24 ore sono stati mediati su diversi giorni ed infine si è ricorso ad un fitting sinusoidale. Ciò è servito ad andare ad individuare durante quale parte della giornata fossero raggiunti i valori di picco per le diverse bande, andando a confrontare i risultati prima della stimolazione e durante la fase cronica.

Infine sono state prese in considerazione le variazioni relative nel potere spettrale della singola banda rispetto al potere spettrale totale e della singola banda prima della stimolazione rispetto alla fase cronica.

Alla fine di questo studio è stato osservato uno sfasamento della modulazione circadiana nel ritmo beta. Ciò ha confermato che lo sfasamento osservato nella fase latente non è un fenomeno transitorio, ma altresì persiste durante la fase cronica, aprendo nuove ed interessanti ipotesi, che saranno illustrate in seguito.

L'organizzazione della tesi è la seguente:

- Introduzione: il capitolo introduce i concetti fondamentali per comprendere lo svolgimento e lo scopo della tesi; in particolare vengono forniti alcuni dati essenziali relativi all'epilessia (sia in generale che piu' approfonditamente sull'epilessia del lobo temporale), ai ritmi circadiani ed all'ippocampo (con particolare attenzione per la regione CA1 e per i principali ritmi EEG ed il loro significato).
- Design Sperimentale: il capitolo descrive il protocollo seguito ed il set-up sperimentale, soffermandosi sugli aspetti principali del modello animale impiegato.
- Analisi dei Dati: il capitolo tratta le metodologie impiegate per l'analisi dei dati sperimentali, fornendo una concisa descrizione delle stesse e soffermandosi sugli accorgimenti necessari per il loro utilizzo in questo progetto.
- Risultati: in questo capitolo sono presentati i risultati dello studio descritto in questa tesi.
- Conclusioni: in questo capitolo i risultati precedentemente illustrati vengono commentati ed alcune ipotesi, da essi scaturite, vengono presentate.
- Sviluppi Futuri: infine, in questo capitolo, sono descritte alcune linee di ricerca che potrebbero essere seguite al fine di acquisire nuove informazioni e di sottoporre a verifica le ipotesi introdotte precedentemente.

CHAPTER 1 INTRODUCTION

This thesis was developed at the Epilepsy Research Lab at the University of Florida and presented at the University of Florida and at Politecnico di Milano as a fulfillment of the Atlantis CRISP (Computing, Robotics and Imaging for Surgery Platform) double-degree exchange program.

Epilepsy

Epilepsy is the most common primary disorder of the brain, and, according to the World Health Organization, is one of the leading causes of neuropsychiatric disability worldwide, along with depression [1]. The word *epilepsy* derives from the Greek verb *επιλαμβάνειν* (*epilambanein*), which means “to be seized” or “to be attacked”. This is due to the fact that, in ancient times, diseases were often seen as attacks by the gods or evil spirits and seizures were the most vivid examples of demonic possession. For the same reason, epilepsy was also called the “sacred disease” [1]. Passing from myth to science, Hippocrates is considered the first one to understand that epilepsy is a brain disease and he proposed that it should have been treated by diet and drugs, rather than by religious practices [1].

Epilepsy is not a specific disease, but a broad category of symptom complexes originating from a number of disordered brain functions, whose insurgence may be due to a number of different pathologic processes (such as brain injuries, tumors and genetic factors) [1]. The common and fundamental characteristic of epilepsy is the presence of recurrent and usually unprovoked seizures, which are the manifestation that arise from excessive, synchronous, abnormal firing patterns of neurons,

predominantly located in the cerebral cortex. Such abnormal activity is usually intermittent and self-limited. Seizures are recurrent episodes of brain dysfunction that manifest themselves as stereotyped alterations in behavior such as generalized convulsions, “dreamy states” and even hallucinations, according to the specific kind of epilepsy. Patients may seize frequently or infrequently, following a cyclic pattern (for example seizing at a specific time of the day, such as during sleep or at arousal) or in some other fashion, but, usually, without any intelligible predictability [1].

However epilepsy is more than seizures: this condition implies a number of factors, which contribute to disability and impaired quality of life. Examples of these factors are social isolation and unemployment, which result in unsatisfactory life standards. For this reasons treatment should focus on more than just preventing seizures in order to be really effective [1].

Gowers was the first to recognize, more than a century ago, that is really often present a seizure-free interval between a causative brain injury and onset of symptomatic epilepsy. This interval, commonly defined “latent”, raises questions about the process of *epileptogenesis*, which is considered to be a dynamic one during which time progressive changes in neuronal excitability, inhibition and recurrent excitation occur[1].

It has been reported since the late 19th century that epilepsy is affected by endogenous clocks, which produce circadian (~24-hr period), ultradian (< 24-hr period) and supracircadian (> 24-hr period) rhythms. One of the most obvious of those is the sleep-wake cycle [2]. Three categories of epilepsy are classified according to the timing of generalized seizures with respect to the sleep-wake cycle: awakening, sleep and

diffuse. The first two categories mean that the seizures are usually observed at the moment of arousal and during sleep, respectively; the latter means that seizures occur in a way that doesn't show any circadian modulation. Up to now, the specific mechanisms underlying these phenomena are poorly understood [2].

Circadian Rhythms

A series of biological functions following daily rhythms has been observed in a number of different animal species. If this rhythmicity is the result of a homeostatic modulation, such can be considered *circadian* (from the Latin *circa dies* that is "approximately a day"). The presence of such internally generated daily modulations implies the existence of a biological clock that can keep track of the time of the day. The existence of such clock, called the *circadian pacemaker*, has been demonstrated by experiments in which the subjects had no environmental clues and so the daily modulation could only be the result of internally generated rhythms [3].

As the name suggests, this rhythms are approximately 24 hours long (24.8 hours for humans), which means that some adjusting mechanism is necessary in order to avoid a slow but inexorable drift away of the subjective time with respect to the external time. Most researchers agree with Pittendrigh's "non-parametric theory of entrainment", which states that the period of the biological clock is not changed and that entrainment is achieved by resetting the pacemaker, according to environmental clues called *zeitgebers* (a German word meaning "time givers"). Being the day/night cycle the easiest environmental clue to think about, it is not surprising that the main zeitgeber is light. Minor ones are temperature, exercise, feeding habits and, according to some researchers, social interactions (non-photic zeitgebers, in contrast with the photic zeitgeber that is light) [3].

Given that the circadian pacemaker exists and is entrained by environmental cues, it is then natural to ask where this structure is located in the human body. It was discovered that the circadian clock is located in the hypothalamus in a region called the suprachiasmatic nucleus, so called because it is placed above the optic chiasm, which is the crossing of the optic nerve. The fact that the clock is positioned in the proximity of nerve bundles carrying visual information is not bewildering, given the importance of the photic zeitgeber. In fact, there is a connection between the retinas and the rostral part of the hypothalamus, the retino-hypothalamic tract, which ends in the SCN [3]. It has to be said that there are theories that imply the existence of different circadian clocks, however none of them disproved the central role of the SCN as a circadian pacemaker, so it is said that the SCN is the master circadian clock, which doesn't exclude the existence of other circadian clocks in the body [3].

Temporal Lobe Epilepsy

Among the many epileptic forms, temporal lobe epilepsy (TLE) is one of the most debilitating, with its diffuse and bizarre psychomotor manifestations [4]. The definition of temporal lobe epilepsy, given in 1985 by the International League Against Epilepsy, is of a condition characterized by recurrent, unprovoked seizures originating from the medial or lateral temporal lobe. This condition was first described in 1881 by John Hughlings Jackson, who recognized seizures originating from the temporal lobe and the "dreamy state" correlated with such [5]. In surgical centers worldwide, TLE is the most common type of localization-related epilepsy [6].

Two different kinds of seizures are associated with TLE: simple partial seizures, which cause no loss of awareness, and complex partial seizures, which cause loss of

awareness. These partial seizures may secondarily generalize, which means that they can spread to a wider portion of the brain [5, 7].

The features of seizures originating from the temporal lobe, even though extremely variegated, have certain common patterns such as a mixture of different feeling, emotions and thoughts and even hallucinations. Such episodes are called “auras” and a description of them has been given by the 19th century Russian writer Dostoyevsky, who suffered from epilepsy himself, in the novel *The Idiot* [7]. Some physicians have hypothesized, retrospectively, that Vincent Van Gogh, the famous Dutch painter, suffered from TLE [4].

According to the classification provided by the International League Against Epilepsy (ILAE), TLE etiologies are divided into symptomatic (cause known), idiopathic (genetic) and cryptogenic (cause unknown) [5].

Hippocampal sclerosis is the most common pathologic substrate in adult patients with temporal lobe epilepsy. This consists of severe neuron loss in specific regions of the hippocampus, such as CA1, prosubiculum, CA4 and hilus; other regions, such as CA2 and CA3, do not appear to be greatly affected by this kind of damage. Hippocampal damage is often bilateral, but usually asymmetric, with greater damage in the epileptic side. Surgical studies showed that hippocampal sclerosis is probably the result of previous brain injury and not the result of repeated seizures. Hippocampal sclerosis is associated with neuronal reorganization, which is typical of epileptic hippocampi and is probably involved in the generation of chronic seizures. The aforementioned reorganization involves excitatory mossy fibers, inhibitory GABAergic axons and fibers with other neurotransmitters, such as somatostatin. It can be said then

that a sclerotic hippocampus is not an inactive region, but instead has probably a role in epileptogenesis [8]. Finally, hippocampal sclerosis is the principal structure responsible for seizures in TLE [9].

Hippocampus

The hippocampus is a subcortical structure that is part of the limbic system (Figure 1-1), which is considered to be concerned with olfactory perception and, at least in humans, emotional behavior. The limbic system is an organization of different anatomical units (hippocampus, amygdala, cingulate gyrus, fornix, thalamus and hypothalamus) with common functions and is located on top of the brainstem, under the cortex. The hippocampus bulges into the temporal horn of the lateral ventricle and its shape resembles the one of a sea horse (Figure 1-2), which explains the name given to this structure.

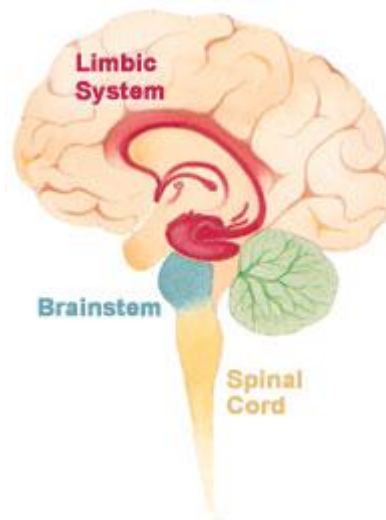


Figure 1-1. Depiction of the limbic system and its position in the brain. Image taken from Wikipedia (Public Domain License).

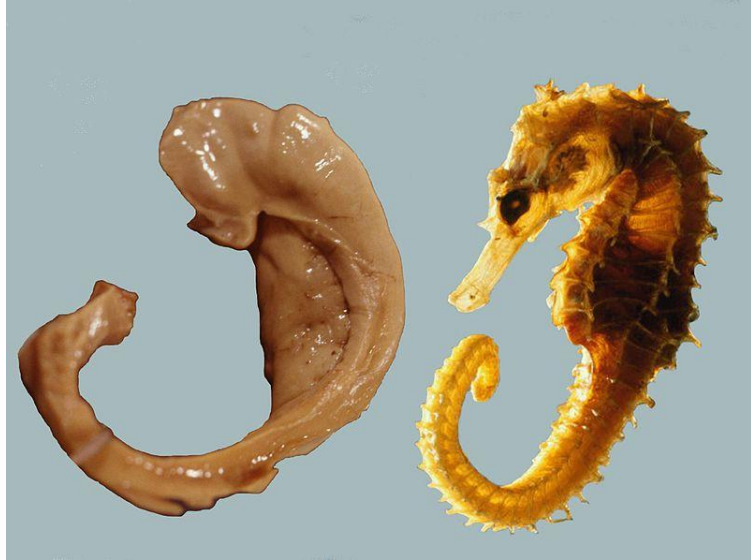


Figure 1-2. Laszlo Seress' preparation of a human hippocampus alongside a sea horse. Image taken from Wikipedia (Creative Commons Attribution-Share Alike 1.0 Generic License).

Anatomy

The hippocampus consists of the cornu Ammonis (or hippocampus proper) and the gyrus dentatus (or fascia dentata), these two laminae are rolled up in a way that resembles two U-shaped structures fitting into one another [10].

The cornu Ammonis can be further divided into four regions, which Lorente de No named CA1, CA2, CA3 and CA4. CA1 continues from the subiculum and its stratum pyramidale is large in humans, but dense and narrow in rats. This field is also said to be a “vulnerable sector” or Sommer sector, due to its sensitivity to hypoxia and to its being the focus for hippocampal damage occurring with epilepsy [10, 11].

CA2 is composed of large, densely packed somata, and so its stratum pyramidale is dense and narrow. CA3 has pyramidal somata similar to those of CA2, but they are less dense; a typical feature of CA3 is the presence of non-myelinated fibers, the mossy fibers, which originates from the gyrus dentatus; furthermore CA3 is said to be a “resistant sector” or Spielmeyer sector, due to its characteristic of being quite resistant

to hypoxia. Finally, CA4 has few large somata scattered among large myelinated mossy fibers typical of this region; this is a sector of medium vulnerability or Bratz sector [10].

Functions

There are several hypotheses regarding the possible functions of the hippocampus and they can be divided in four categories: (I) learning and memory, (II) regulation of emotional behavior, (III) aspects of motor control and (IV) regulation of hypothalamic functions [10].

It is generally accepted that the hippocampus has a critical role in learning and memory; in fact, clinical observations show that, in humans, hippocampal damage causes memory disorders, in particular short-term memory. The hippocampus takes part in all aspects of the declarative memory: semantic memory (memory of concepts), episodic memory (memory of events) and spatial memory (spatial location recognition). The hippocampal neurons have a remarkable plasticity that is the cause of long term potentiation: a persistent modification of the neuronal physiological state due to repetitive stimulation. The information to be memorized passes through the hippocampus and is then stored in the association cortex; this idea is supported by the fact that it has been shown, using PET and fMRI, that the hippocampus projects to large neocortical areas, including the prefrontal and retrosplenial cortices [10].

Starting with the studies of Papez (1937), the regulation of emotional behavior has been considered one of the main functions of the hippocampus; nowadays such functions are considered to be mainly carried out by the amygdala, though. This doesn't mean, however, that the hippocampus is not concerned with emotional behavior at all; in fact it is accepted that it has a role in the regulations of some emotional behavior, in particular the one connected to pain [10].

The hippocampus is believed to be involved in the ventral striatal loop, which may participate in the control of motor behavior, in particular motor reactions to emotion [10].

Finally, the hippocampus is involved in the regulation of the hypothalamo-hypophyseal axis [10].

EEG Rhythms

Different EEG rhythms can be observed in the hippocampus: theta or rhythmic slow activity (3-11 Hz), beta (12-29 Hz) and gamma (30-70 Hz) [12, 13]. It is believed that each EEG pattern has specific behavior correlates [14].

Theta rhythms occur during translational movements, arousal and attention and during REM sleep [14]. Three main functions have been hypothesized for theta. The first of which is a global synchronizing mechanism that locks the whole hippocampus into a global processing mode and organizes the activity of each of its region with respect to the others [14]. Second, theta rhythm provides a clocking system for the timing of hippocampal spikes; different responses have been reported, according to the timing at which information reaches the hippocampus with respect to the underlying theta rhythm [14, 15, 16, 17, 18, 19, 20]. The third function is to provide temporal control over long-term potentiation and so over the storage and retrieval of information [14, 15, 16]. The direct involvement of theta rhythm in long-term storage was indicated by studies showing a severe memory deficit after the selective elimination of theta oscillations, achieved by septal lesions [15].

The behavioral correlates of beta activity are not clear: in the rat, beta waves can be elicited by olfactory inputs linked to the presence of predators. It was observed that seizures induce an increase in beta activity [14]. It has been also hypothesized that beta

rhythm might be used for high-level interactions involving distant structures that can't be directly reached through gamma synchronization [13].

It is thought that gamma synchronization is necessary to bind together elements of complex representation [13, 14], and it was even hypothesized that such synchronization is necessary for the normal functioning of the waking brain [21]. Possible functions of the gamma oscillations are coincidence detection, synaptic plasticity and phase encoding [21].

CA1 Region

The CA1 region is of particular interest for several reasons. First, it is the main source of output from the hippocampus and its computational importance is suggested by the anatomy (there are approximately 10^{10} synapses projecting from CA3 to CA1) [22, 23]. Second, for its role in long-term potentiation [15] and in TLE [8, 10]. Third, it is the most frequent location for hippocampal recordings [11, 22, 24].

The CA1 area receives excitatory inputs from the entorhinal cortex and CA3, and inhibitory inputs from basket cells and the oriens-alveus/lacunosum-moleculare [24].

There are several hypotheses on the functions of CA1. The first hypothesis is that it acts as a relay, ensuring efficient information transfer from CA3 to the neocortex [22, 25, 26]. The second hypothesis is that it detects novel stimuli by comparing CA3 output and cortical input [22, 27, 28]. The third hypothesis is that CA1 acts as a predictor of places and events, based on previous knowledge, by comparing activity in CA3 with cortical input [22, 29]. The fourth hypothesis claims that CA1 is involved in multiple memory loops [22, 30].

Research Goal

Recent studies carried out in this lab have shown a phase-shift in the circadian modulation of EEG features in the CA1 region in an animal model of TLE, during the latent period of the disease [31, 32, 33]. This study, extending from there, aims at investigating the presence of a similar phase-shift during the chronic phase of the disease. In particular, this project focuses on the circadian modulation of the power spectrum of frequency bands with physiologic relevance (theta, beta and gamma waves).

Thesis Overview

In Chapter 2 the experimental design will be discussed, describing the animal model employed, the protocol followed and the electrode placement.

In Chapter 3 the methods employed to analyze the intra-hippocampal EEG signal in order to investigate the circadian modulation will be described.

Chapter 4 will be dedicated to the presentation of the results of this study.

In Chapter 5 the results shown in Chapter 4 will be discussed, providing hypothesis on their possible interpretation and significance.

Finally, Chapter 6 will deal with the future developments and improvements of the study described in this thesis.

CHAPTER 2 EXPERIMENTAL DESIGN

Animal Model

For this study, an animal model of chronic limbic epilepsy, which is characterized by recurrent spontaneous seizures, after an episode of limbic status epilepticus [34, 35, 36], was adopted.

The episode of limbic status epilepticus that triggers the development of the disease into the chronic phase is achieved by continuous hippocampal stimulation, which yields a self-sustaining limbic status epilepticus [37].

The temporal evolution and the electrographic characteristics of this model have been reported to be consistent with the ones observed in human patients affected by temporal lobe epilepsy with hippocampal sclerosis [34].

Protocol Followed

Nine adult male Sprague Dawley rats of age 63 days and weighing between 200 and 265 grams, were considered for this study. The animals were implanted with electrodes bilaterally in the hippocampus and they were housed, each in its own cage, at a room temperature of 25°C in a controlled environment with 24 hour symmetric day-night cycle (lights on at 6 am, lights off at 6 pm), so that environmental factors could be ruled out as a cause of the circadian phase-shift, if present. The animals were continuously monitored with both video and electrical activity recordings for an average period of 5 weeks, in order to identify spontaneous seizures. After a week of baseline recordings, the 7 of the 9 animals that survived the surgery have been continuously electrically stimulated (400µA at 50 Hz for 50-70 minutes) with the intent of inducing brain injury that would lead to chronic spontaneous seizures. Only 3 of these 7 animals

developed the chronic condition, with seizure of Racine grade 3 or higher; the other 4 either didn't seize or dislodged their head-stages. Once the recording session was over, the animals were sacrificed and their brains extracted and imaged in order to confirm the location of the electrodes.

Surgery and Electrode Implantation

All the procedures have been approved by the Institutional Animal Care and Use Committee of the University of Florida (IACUC protocol D710).

The animals were completely anesthetized with the injection of 10 mg/Kg (0.1 mL by volume) of xylazine and kept in that state with the inhalation of isoflurane (1.5%). The skull was then exposed by a mid-sagittal incision and a 16 microwire electrode (50 μ m, Tucker-Davis Technologies, Alachua, FL) array, consisting of two rows separated by 500 μ m and with a spacing of 250 μ m between two adjacent electrodes, was placed bilaterally over the CA1-CA2 and dentate gyrus. The furthest left microwire was 4.4 mm caudal to bregma, 4.6 mm left of midline suture and at a depth of 3.1 mm from the dura. The second microwire array was placed to the right of midline suture in a diagonal way. The furthest right microwire was 3.2 mm caudal to bregma, 2.2 mm to the right of midline suture. The closest right microwire was 5.2 mm caudal to bregma, 1.7 mm to the right of midline suture and at a depth of 3.1 mm from the dura. A bipolar, twisted, Teflon-coated, stainless steel electrode (330 μ m) was implanted in the right posterior ventral hippocampus (5.3mm caudal to bregma, 4.9 mm right of midline suture and at a depth of 5 mm from the dura), to provide the electrical stimulation necessary to induce the brain injury (Figure 2-1). To anchor the electrode arrays to the skull four 0.8 mm stainless steel screws (two for each electrode array) were used. Of each pair of screws one (2 mm to the bregma and bilaterally 2 mm) served as the ground electrode and the

other (2 mm to the lambdoidal suture and bilaterally 2 mm) as the reference electrode. The whole surgical area was finally closed and secured with cranioplast cement and the animals were allowed to recover for a week before the starting of the recording session.

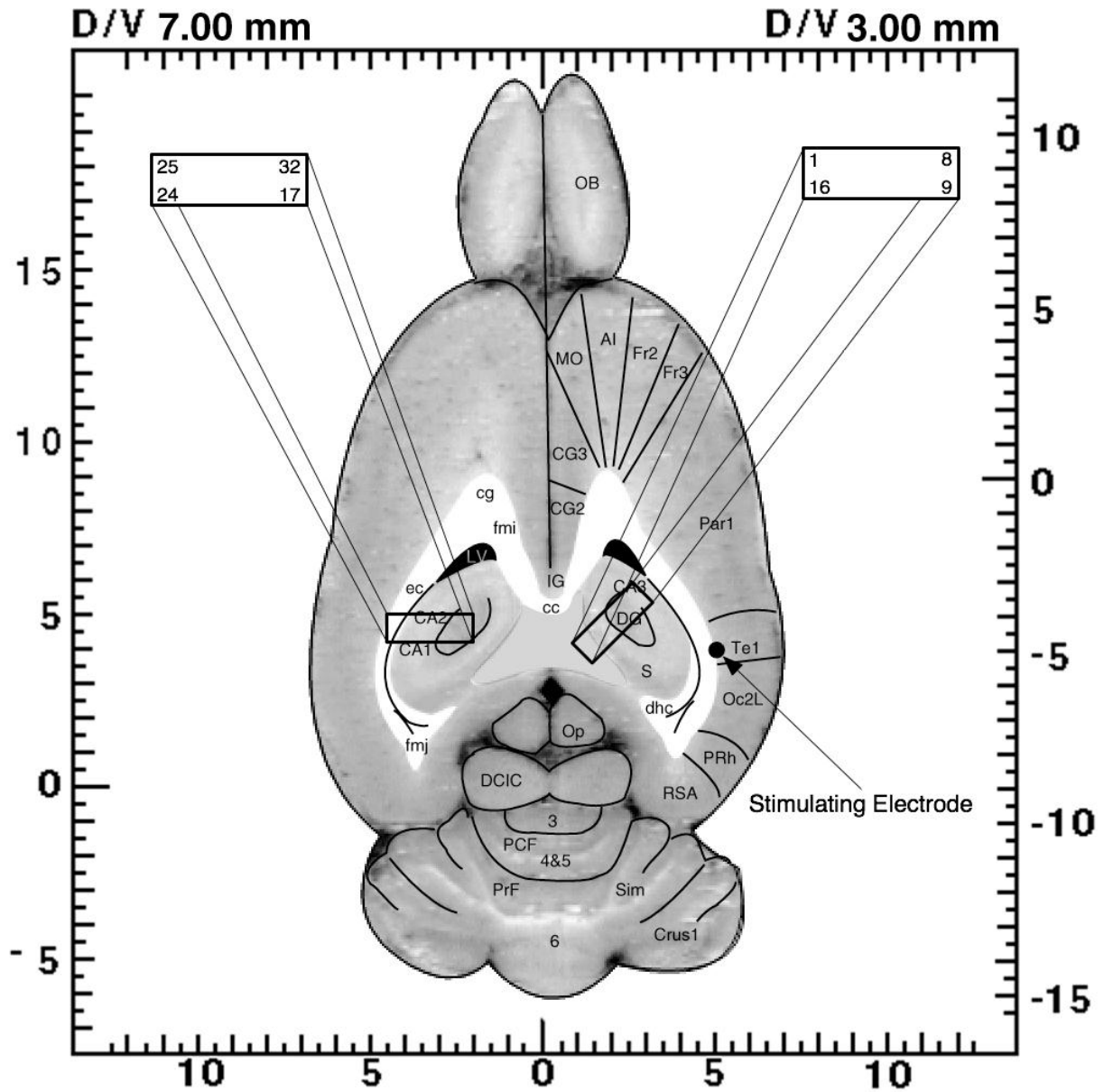


Figure 2-1. Placement of the two 16 microwire electrode arrays and of the stimulating electrode.

Electrical Stimulation

To induce status epilepticus, 7 of the 9 rats (the ones which survived the surgery) underwent continuous electrical stimulation. A biphasic square wave stimulus at a frequency of 50 Hz and with a pulse width of 1 millisecond and intensities of 300-400 μ A was applied continuously for 50-70 minutes with a duty cycle of 10 seconds on and 2 seconds off.

After 20-30 minutes of stimulation, the animals showed convulsive seizures, manifesting themselves as “wet dog shakes”, up to 1 minute in duration, every 10 minutes. After the end of the stimulation continuous EEG recordings were observed for electrographic evidence of seizures in the following hours. When the animals stabilized showing no more signs of abnormal electrographic activity, they were brought back to the vivarium and kept there for 4-6 weeks, during which 3 of the 7 animals developed spontaneous seizures of a minimum Racine grade of 3. So, all the data considered for this study comes from this 3 rats that entered the chronic phase of the disease.

Data Acquisition

Each rat was connected to a 32-channel commutator for the continuous EEG recordings. The output of such device was fed into the recording system, which consisted of two 16-channel pre-amplifiers and a 16-bit A/D converter with a sampling rate of 12 KHz. The digitized signal was then band-pass filtered between 1.5 Hz and 7.5 KHz by a Pentusa RX-5 data acquisition board (Tucker-Davis Technologies, Alachua, FL). The band-passed digital stream was finally stored in binary process for later processing.

High Resolution MRI

The animals were perfused with formalin (10% concentration) and their brains were extracted and soaked in phosphate buffer solution for 24 hours in order to remove any residual fixative. After this, the brain was kept in a tube containing fluorinated oil (Fluorinert, 3M Corp., Saint Paul, MN) and imaged at 17.6 T with a Bruker (Billerica, MA) Avance MRI machine in order to verify the correct positioning of the electrodes.

Images were acquired with a 3D gradient echo pulse sequence with a repetition time of 150 milliseconds, gradient echo time of 15 milliseconds. The field-of-view of the image was 30 mm × 15 mm × 15 mm in a matrix of 400×200×200 pixels, with a resolution of 75 × 75 × 75 μm³. A tri-dimensional image was reconstructed applying a 3D Fourier transform.

CHAPTER 3 DATA ANALYSIS

This study focused on spectral features of the intra-hippocampal EEG signal, acquired from the electrode placed in the CA1 region. After having extracted the spectrum of the signal, this was de-trended and divided in 24-hour long cycles, which were then averaged. The 24-hour cycle resulting from this operation was then fitted to a sinusoid of period 24 hours and the time at which the positive peak was reached was identified manually from the generated plots. In addition to that, the relative power of each band was calculated as the ratio of the power of the considered band with respect to the sum of the power of all the bands. Furthermore, the relative variation in the relative power post-injury with respect to pre-injury was calculated as the ratio of the power of the considered band after in the chronic phase with respect to the power of the same band before injury. Finally the total power was considered. The details of each of these operations will be described.

Extraction of the Spectra

To evaluate the frequencies present in the signal the discrete Fourier transform was employed. Shortly, the Fourier transform decomposes a waveform into a sum of sinusoids of different period and amplitude. The discrete Fourier transform is the implementation of the Fourier transform in discrete time, which means with a finite number of points rather than with a continuous function.

The discrete Fourier transform maps a sequence of points $x(n)$ in the time domain into the frequency domain. The mathematical definition of the DFT is given in Equation 3-1 [38].

$$X^F(k) = \sum_{n=0}^{N-1} x(n)W_N^{kn}, \quad k = 0, 1, \dots, N-1, N: DFT \text{ coefficients}$$

$$W_N^{kn} = e^{\frac{-j2\pi kn}{N}} \quad (3-1)$$

Where $x(n)$, $n=0, 1 \dots N-1$, is a uniformly sampled sequence, with sampling interval T . $X^F(k)$ is the k -th DFT coefficient.

The DFT has many applications, among which are the processing of biological signals such as EKG and EEG [38]. So, the analysis performed in this study employs techniques which are well established in the field.

The Fourier transform assumes that the signal considered is stationary and that the signal in the sample repeats infinitely [39]. However, the EEG signal is non-stationary, in general; to solve this issue it is possible to divide the EEG signal in short chunks over which the hypothesis of stationarity can be assumed to be true [40, 41, 42]. In this study the signal has been broken down in 10 seconds long sequences [43, 44] with a 50% overlap.

Before the application of the DFT a Hamming window was applied. The Hamming window is designed in order to minimize the maximum side-lobe [45], the reason for doing this is the reduction of the artifacts arising from the abrupt transitions from the end of a chunk to the beginning of the same chunk, due to the hypothesis of periodicity of the signal assumed by the Fourier transform. The mathematical definition of the Hamming window is given in Equation 3-2 [46] and an example of its shape is given in Figure 3-1 [45].

$$w(n) = 0.5 \left(1 - \cos\left(\frac{2\pi n}{N-1}\right) \right) \quad (3-2)$$

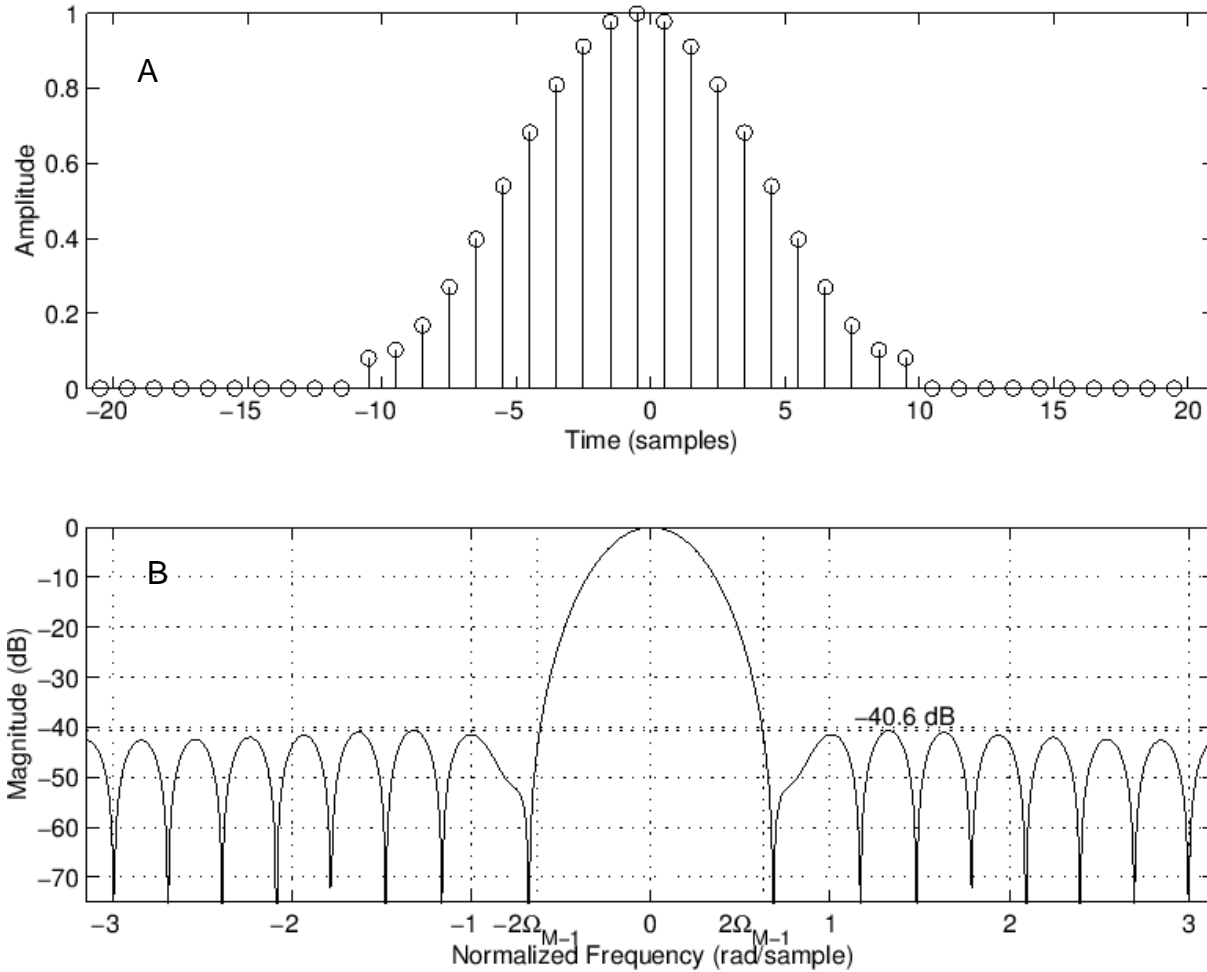


Figure 3-1. The shape of a Hamming window and of its transform. $M = 21$ A) Hamming window. B) transform.

The reason for the 50% overlapping of the 10 seconds windows is to compensate for the fact that the Hamming windows attenuates the amplitude of the time samples at the extremities of the chunk considered.

The spectra of the 10 seconds long chunks were averaged over an hour, yielding the hourly estimate of the spectral power of each band considered. This was done over a length of 4-6 days, yielding a series of points each of which represents the hourly value of the spectral power in the considered band (Figure 3-2). This procedure was

done both before the injury and in a seizure-free period during the chronic phase of the disease.

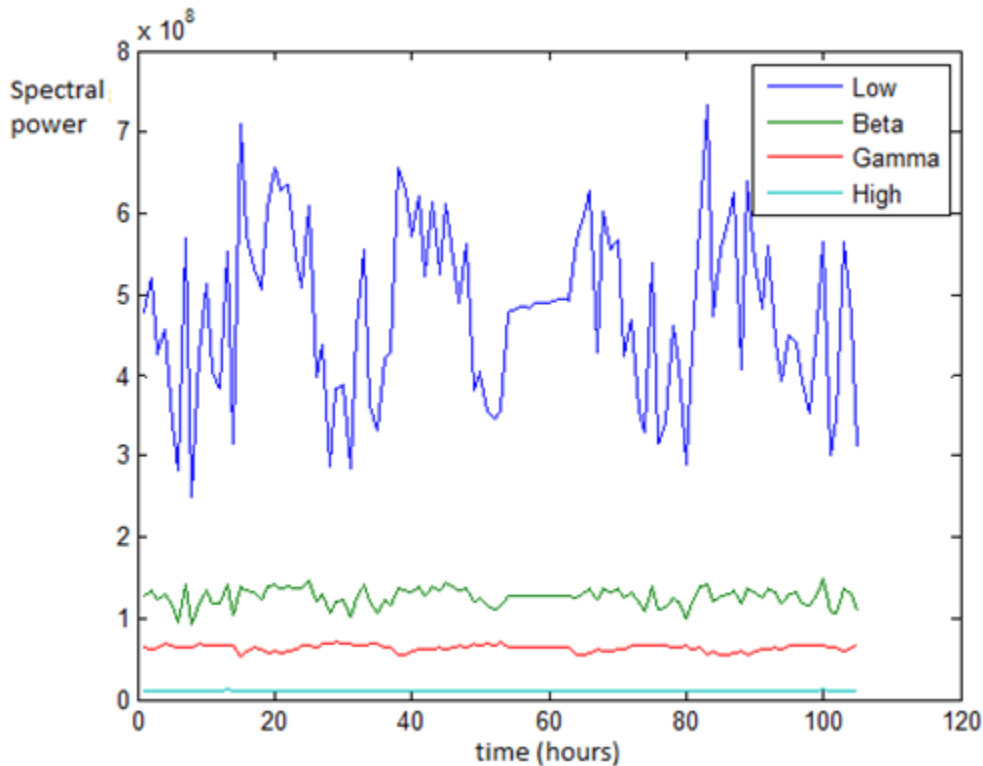


Figure 3-2. Example of plot of the hourly spectral values for the four bands considered.

De-trending

To remove the effects of the supra-circadian rhythms, the data obtained applying the procedure described above has been de-trended. To do so from each point was subtracted the average of the following 48 points, which means 48 hour. This decision is justified by the fact that, considering two complete periods, the average of the circadian modulation over those 48 hours is equal to zero, assuming a sinusoidal circadian modulation, and so the result of the performed averaging is the average supra-circadian variations in the 48 hours following the time point considered.

Numerical examples to prove the efficacy of such an approach, under the given assumptions are presented as follows:

Let's consider a signal composed by the sum of a linear function ($y=0.01x+5$) and a sinusoid of period 50 ($y=\sin(2\pi x/50)$), shown in Figure 3-3. Subtracting from each point the average of the following 100 (that is 2 periods) a sinusoid of period 50 with zero average is obtained, as can be seen in Figure 3-4.

This showed that the approach followed is able to remove the effects of the drift of the baseline, due to supra-circadian modulation.

An example of de-trended data used in this study is provided in Figure 3-5.

Since, in order to de-trend, it is necessary to have data for the following 48 hours, the length of the de-trended data is 2-4 days.

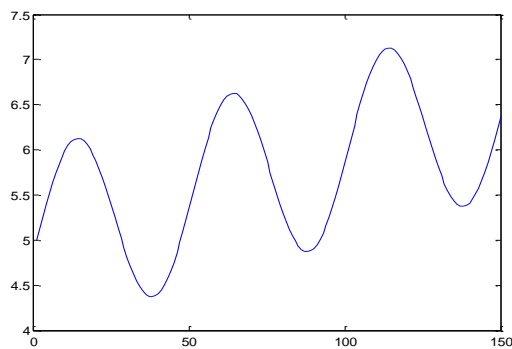


Figure 3-3. Example of a signal composed by the sum of a straight-line and a sinusoid

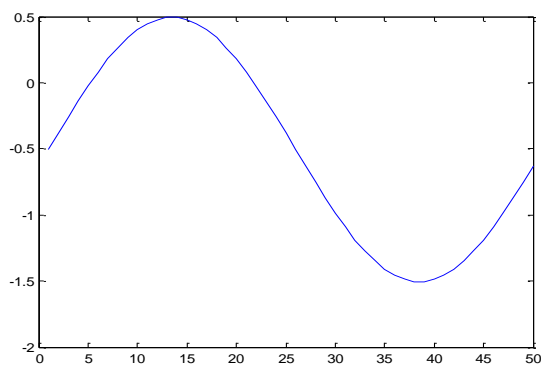


Figure 3-4. Example of the sinusoid obtained from the de-trending of the signal shown in Figure 3-3, using the technique described above.

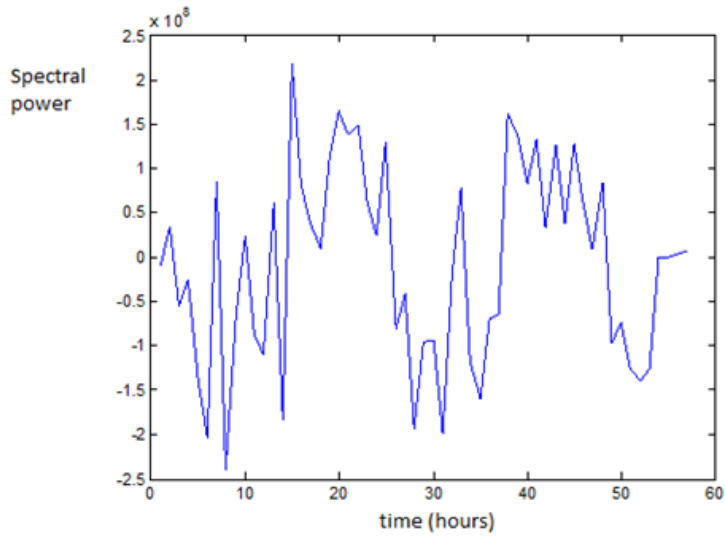


Figure 3-5. Example of de-trended data from this study.

Averaging

The de-trended data has been divided in 24 hour long segments and they have been averaged, in order to enhance the underlying circadian modulation by attenuating the effects of transitory activity and noise. An example of such an operation done with data used in this study is provided below in Figures 3-6, 3-7 and 3-8. Note that the values on the time axes do not correspond to the time of the day they refer to.

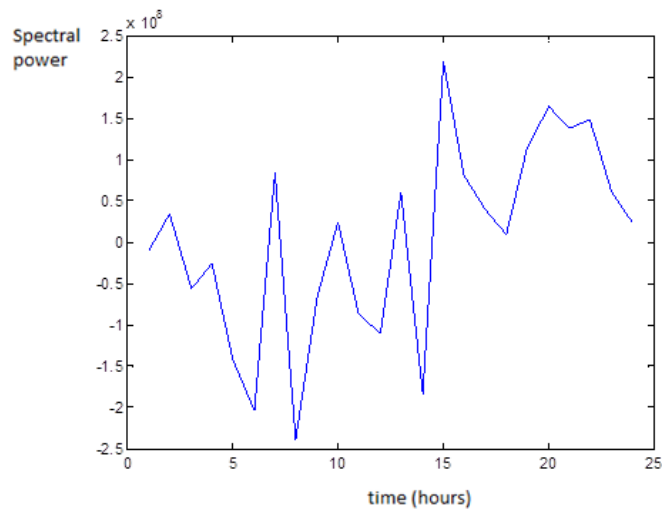


Figure 3-6. Example of de-trended 24 hour long data

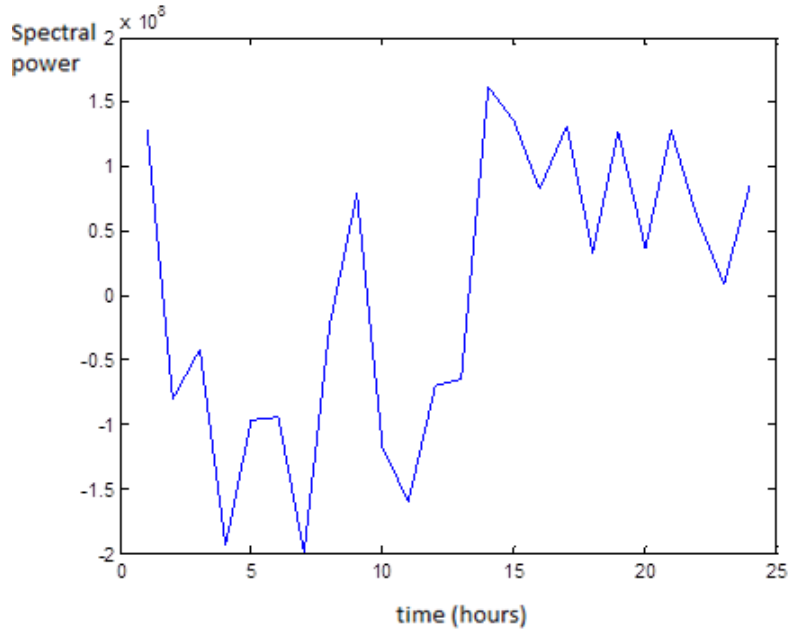


Figure 3-7. 24 hour long segment following the one showed in Figure 3-6

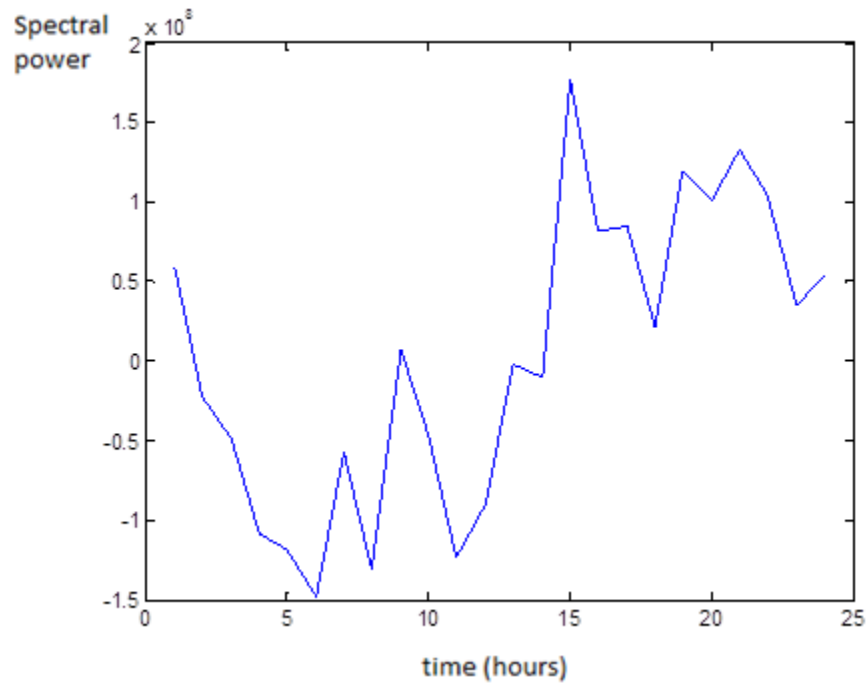


Figure 3-8. Average of the two 24 hour long de-trended segments showed in Figures 3-6 and 3-7

Sinusoidal Fitting

Since it was hypothesized a sinusoidal modulation of the circadian rhythms, the de-trended and averaged data has been fitted with a sinusoid of period 24 hours. This was done employing an algorithm that minimizes the squared error between the experimental data and the fitting function. The fitting function used is given in Equation 3-3. An example of the fitting sinusoid superimposed to the experimental data is shown in Figure 3-9.

$$f(x_1, x_2, x_{data}) = x_1 \sin\left(\frac{2\pi x_{data}}{24} + x_2\right) \quad (3-3)$$

Where x_1 and x_2 are the free parameters (amplitude and phase of the sinusoid) and x_{data} is the experimental data.

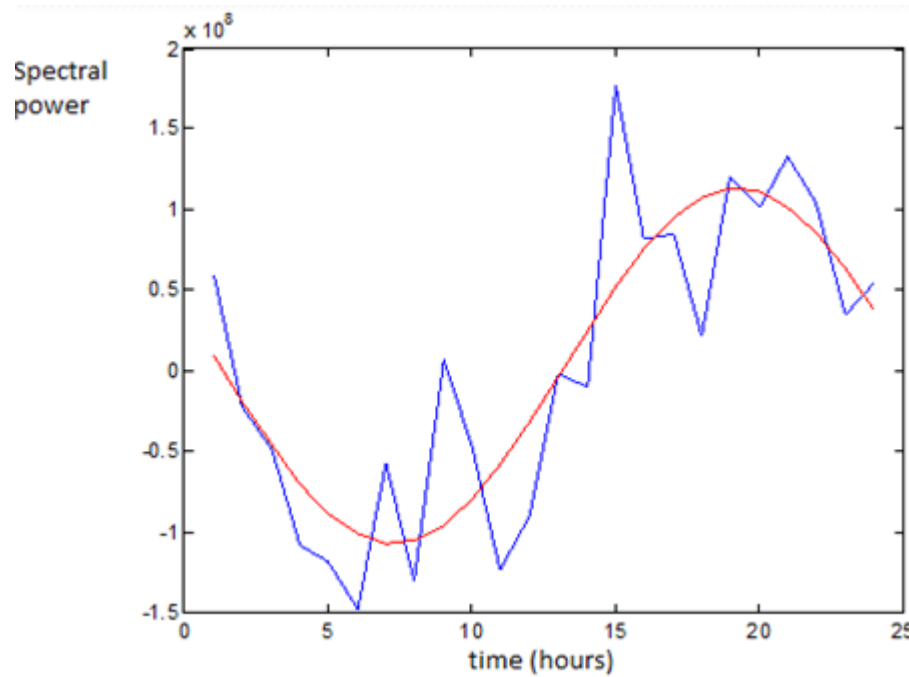


Figure 3-9. Example of the superposition of the fitting sinusoid to the experimental data

Relative Power

In addition to the analysis of the power spectra of the four bands described above, the relative power of each band with respect to the sum of all the bands has been calculated and its variations during the day have been considered. Furthermore the variations in the relative power for a given time of the day between the pre-injury and chronic phase have been considered. The calculation performed to evaluate the relative power is described in Equation 3-4.

$$RP_{i,k} = \frac{P_{i,k}}{\sum_i P_{i,k}} \quad (3-4)$$

Where RP is relative power, $i=1,2,3,4$ is the index relative to the band considered, $k=1,2,\dots,24$ is the index relative to the time of the day considered and P is the spectral power.

The relative power has been evaluated using Equation 3-4 on 3-5 days of data, each yielding a 4x24 matrix containing the values for each band at each time of the day. The data contained in these matrices has been averaged, giving a 4x24 matrix containing the averaged relative power values.

The relative variation of the relative power for a given band at a given time of the day between the pre-injury and chronic phase has been calculated using Equation 3-5.

$$RVRP_{i,k} = \frac{RP_{i,k}(chronic)}{RP_{i,k}(pre)} \quad (3-5)$$

Where RVRP is relative variation of relative power, indexes i,k are the same as the ones described for Equation 3-4 and RP is the averaged relative power. To make the data more intelligible only the variations of a certain entity were taken into account. In particular, only the ones who were higher than 10 and 25 percent of the mean relative power for a given band, when evaluating the daily variations of relative power, and the

ones who were higher than 10 and 25 percent of the pre-injury value, when evaluating the variations in relative power between pre-injury and chronic phases.

The results with both these two threshold values (10% and 25%) will be provided in Chapter 4.

Total Power

Finally, the total spectral power has been taken into account. This was calculated as the sum, hour by hour, of the averaged spectral power of all the bands (Equation 3-6).

$$TP_k = \sum_i P_{i,k} \quad (3-6)$$

Where TP is total power, P is spectral power and indexes i, k are the same as before. In this way the total power consists of a vector of 24 points, which was then fitted to a sinusoid of period 24 hours as done before for the power of the single frequency bands.

CHAPTER 4 RESULTS

Here the results of this study will be shown and briefly described. All the comments about their relevance and interpretation will be done in Chapter 5.

Peak Times of the Different Frequency Bands

The results shown below refer to rat #1.

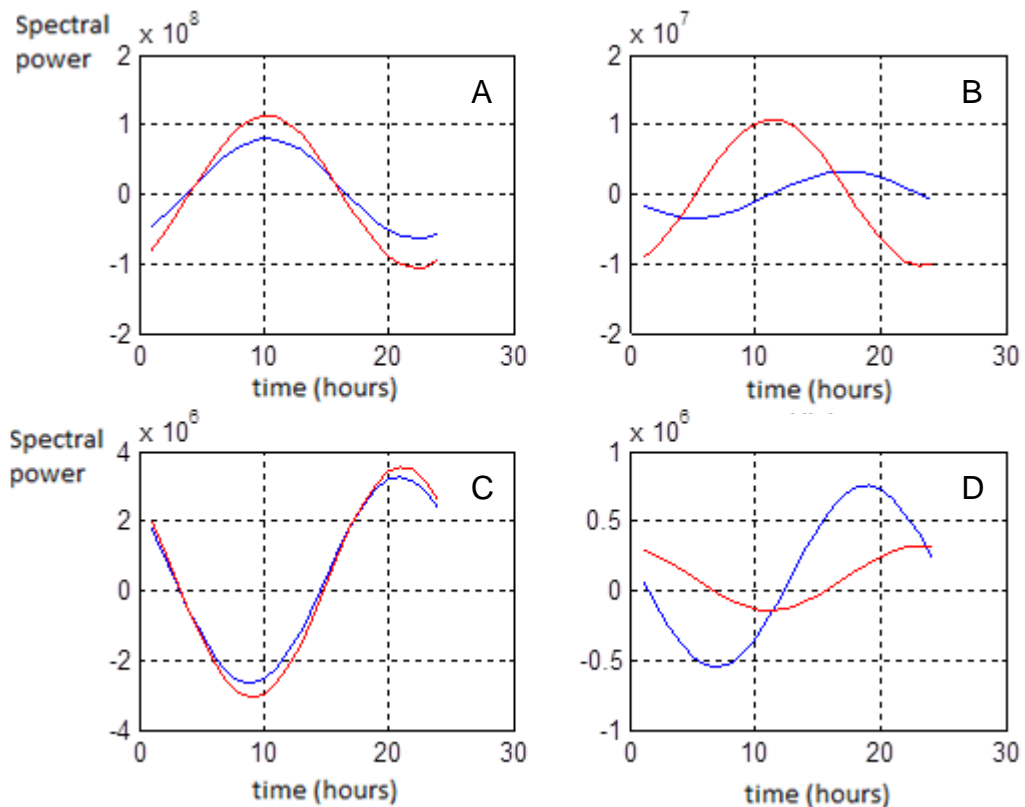


Figure 4-1. Comparison of the circadian modulation for the four different frequency bands before injury (red) and in the chronic phase (blue). The time of day is expressed so that 1 corresponds to 1 am and 24 to midnight. A) Low B) Beta C) Gamma D) High

Before injury the low band peaks at 10, the beta at 11, the gamma at 21 and the high at 23. After injury the low band peaks at 10, the beta at 17, the gamma at 21 and the high at 19.

The results shown below refer to rat #2.

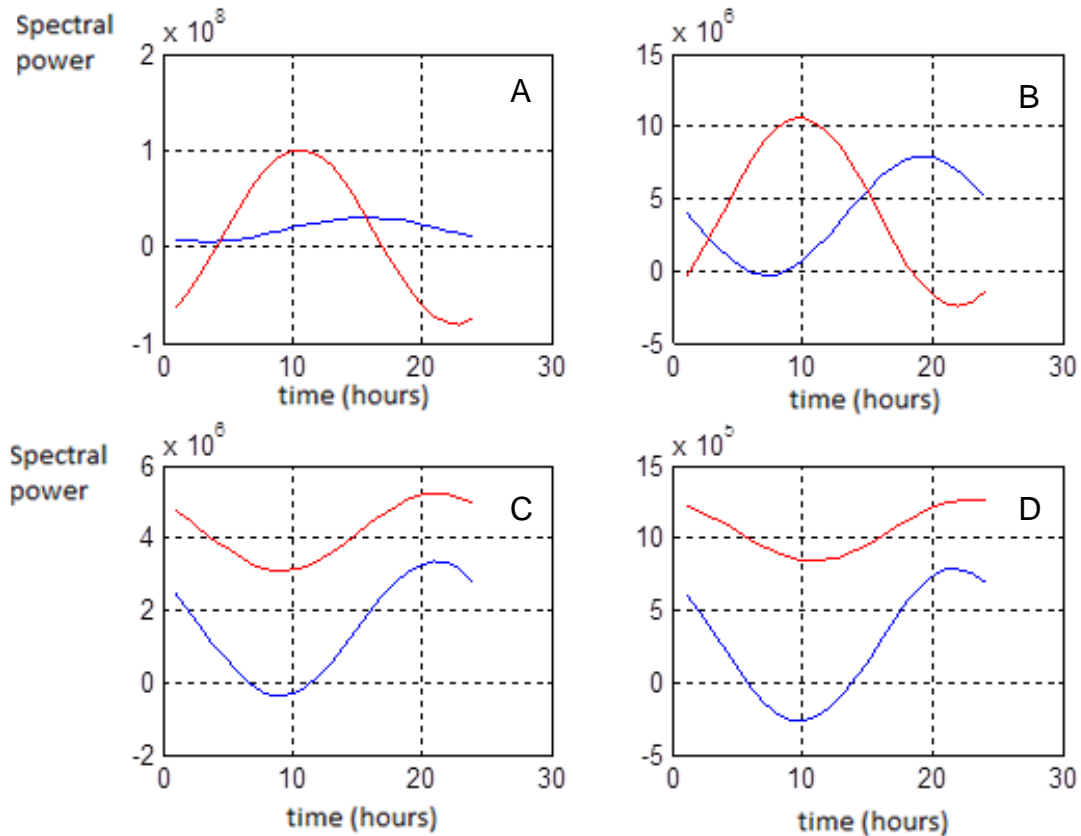


Figure 4-2. Comparison of the circadian modulation for the four different frequency bands before injury (red) and in the chronic phase (blue). The time of day is expressed so that 1 corresponds to 1 am and 24 to midnight. A) Low B) Beta C) Gamma D) High

Before injury the low band peaks at 11, the beta at 10, the gamma at 21 and the high at 23. After injury the low band peaks at 16, the beta at 19, the gamma at 21 and the high at 22.

The results shown below refer to rat #3. Before injury the low band peaks at 10, the beta at 13, the gamma at 16 and the high at 20. After injury the low band peaks at 11, the beta at 16, the gamma at 18 and the high at 21.

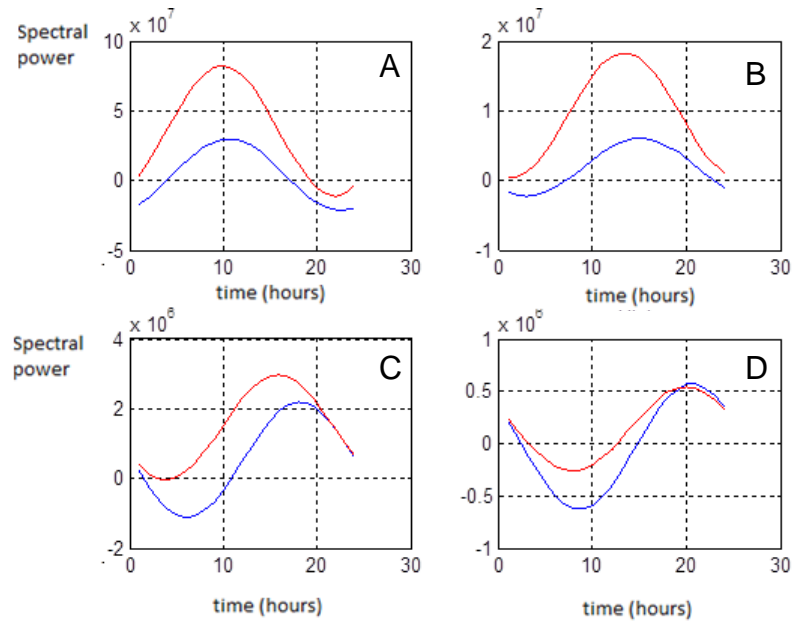


Figure 4-3. Comparison of the circadian modulation for the four different frequency bands before injury (red) and in the chronic phase (blue). The time of day is expressed so that 1 corresponds to 1 am and 24 to midnight. A) Low B) Beta C) Gamma D) High

A summary of the results is given in Tables 1, 2 and 3 and in Figure 4-4.

Table 4-1. Peak times pre-injury for all the bands for all the rats and average values

	Rat #1	Rat #2	Rat #3	Avg pre
Low	10	11	10	10.33
Beta	11	10	13	11.33
Gamma	21	21	16	19.33
High	23	23	20	22.00

The low and beta bands peak in the morning on average, while the gamma and high bands peak in the evening.

Table 4-2. Peak times post-injury for all the bands for all the rats and average values

	Rat #1	Rat #2	Rat #3	Avg post
Low	10	16	11	12.33
Beta	17	19	16	17.33
Gamma	21	21	18	20.00
High	19	22	21	20.67

The low band peaks around noon, while the beta, gamma and high bands peak in the evening.

Table 4-3. Difference in the peak times for all the bands for all the rats and average values.

Post-Pre	Rat #1	Rat #2	Rat #3	Avg post
Low	0	5	1	2.00
Beta	6	9	3	6.00
Gamma	0	0	2	0.67
High	-4	-1	1	-1.33

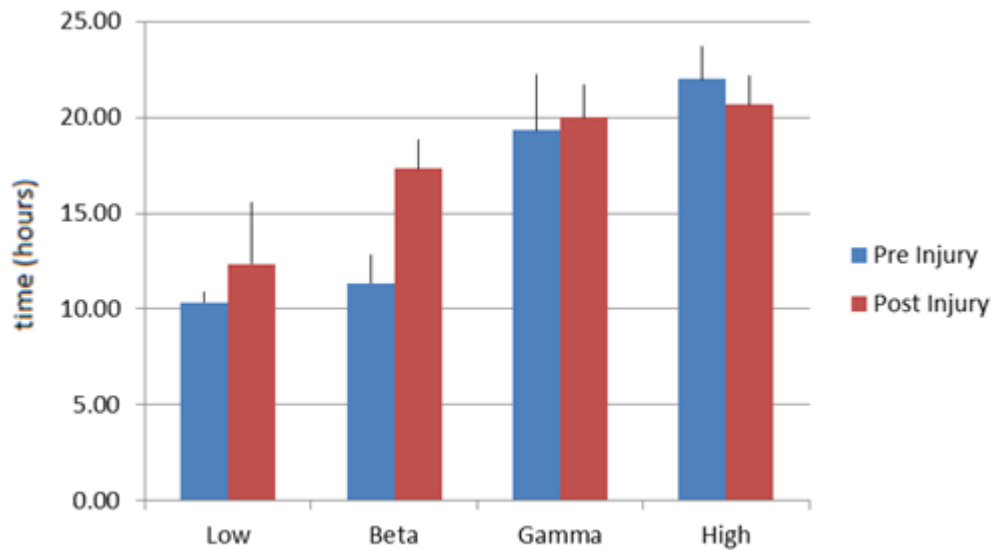


Figure 4-4. Column graph representing the peak time for each band pre injury and post injury. On the y axis time of the day, where 1 is 1 am and 24 is midnight. The error bars are expressed in terms of standard deviation.

It can be seen that only in the beta band there is a change bigger than 3 hours (that corresponds to a phase shift of $\pi/4$). Furthermore, only the difference in peak time of the beta band is statistically significant ($p < 0.05$, evaluated through a paired t-test).

Relative Power

Daily Variations

In this paragraph the variations in the relative power during the day are presented for all the bands for all the rats both pre-injury and in the chronic phase.

The results shown below refer to rat #1. In Figures 4-5 and 4-6, the variations in relative power higher than 10% are shown.

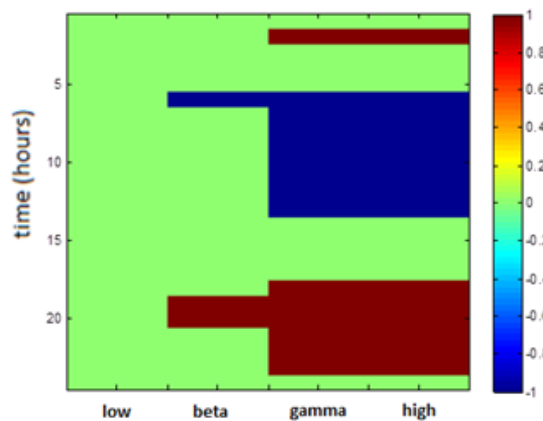


Figure 4-5. Distribution during the day of the variations in the relative power pre-injury. In red increases of more than 10%, in blue decreases of more than 10%. On the y-axis is the time of day, expressed so that 1 corresponds to 1 am and 24 to midnight.

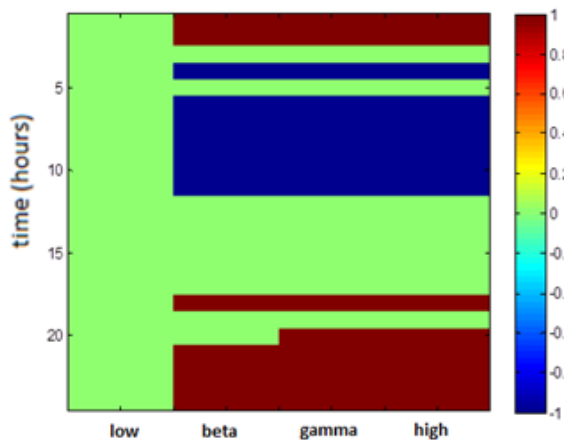


Figure 4-6. Same as Figure 4-5, but after injury

In Figures 4-7 and 4-8, the variations in relative power higher than 25% are shown.

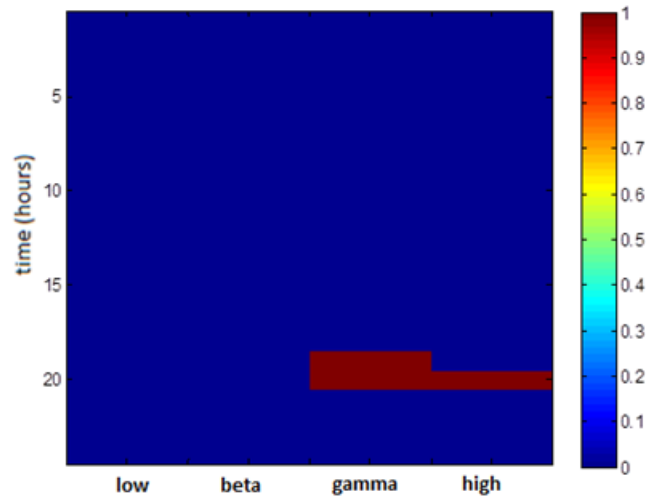


Figure 4-7. Distribution during the day of the variations in the relative power pre-injury. In red increases of more than 25%. On the y-axis is the time of day, expressed so that 1 corresponds to 1 am and 24 to midnight.

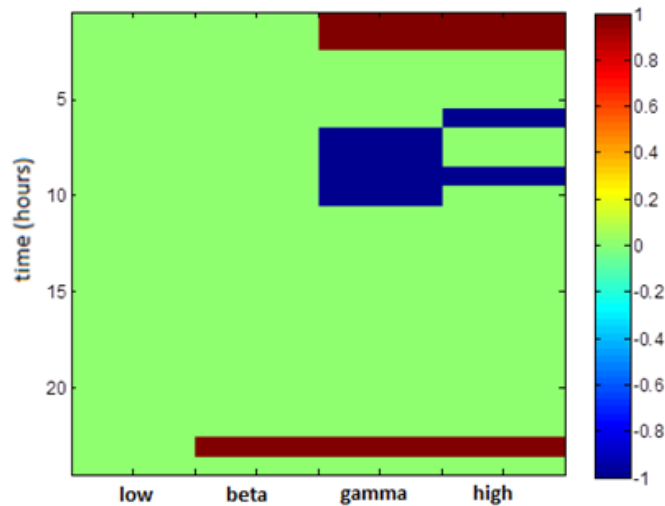


Figure 4-8. Same as Figure 4-7, but after injury

The results shown below refer to rat #2. In Figures 4-9 and 4-10, the variations in relative power higher than 10% are shown, while in Figures 4-11 and 4-12, variations higher than 25% are considered.

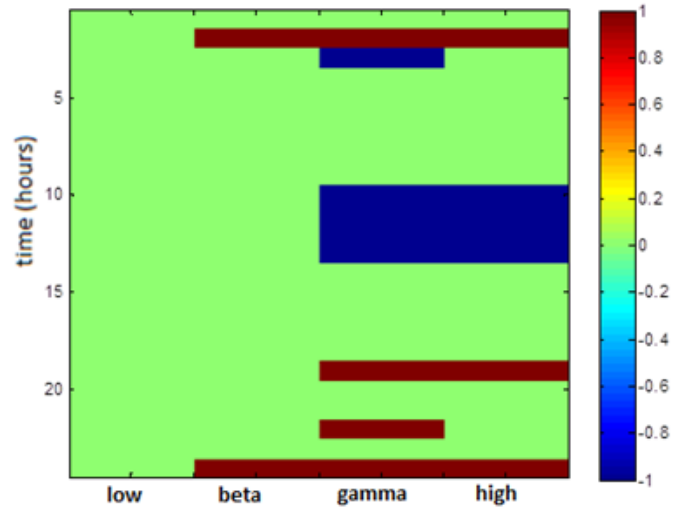


Figure 4-9. Distribution during the day of the variations in the relative power pre-injury. In red increases of more than 10%, in blue decreases. On the y-axis is the time of day, expressed so that 1 corresponds to 1 am and 24 to midnight.

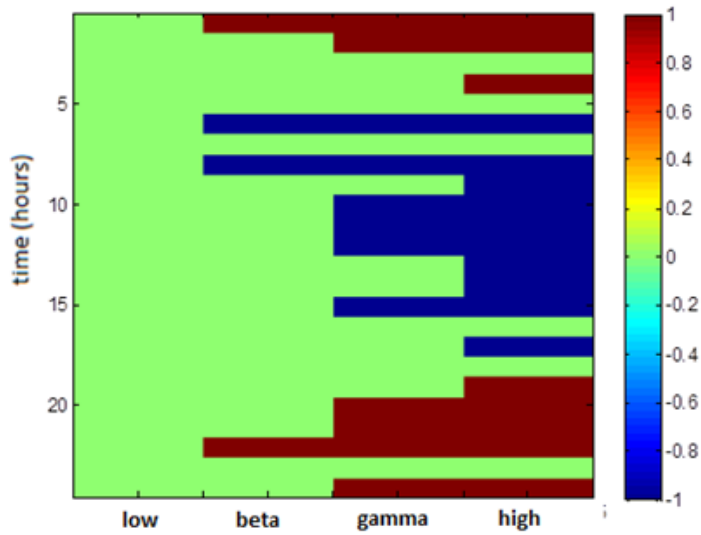


Figure 4-10. Same as Figure 4-9, but after injury

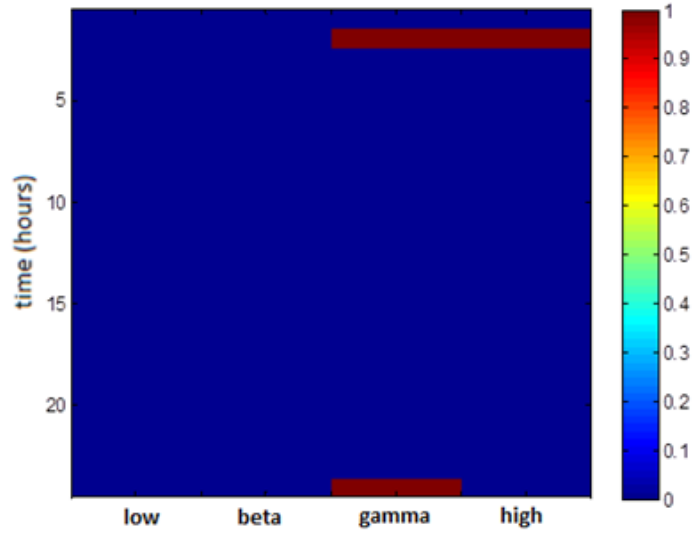


Figure 4-11. Distribution during the day of the variations in the relative power pre-injury. In red increases of more than 25%. On the y-axis is the time of day, expressed so that 1 corresponds to 1 am and 24 to midnight.

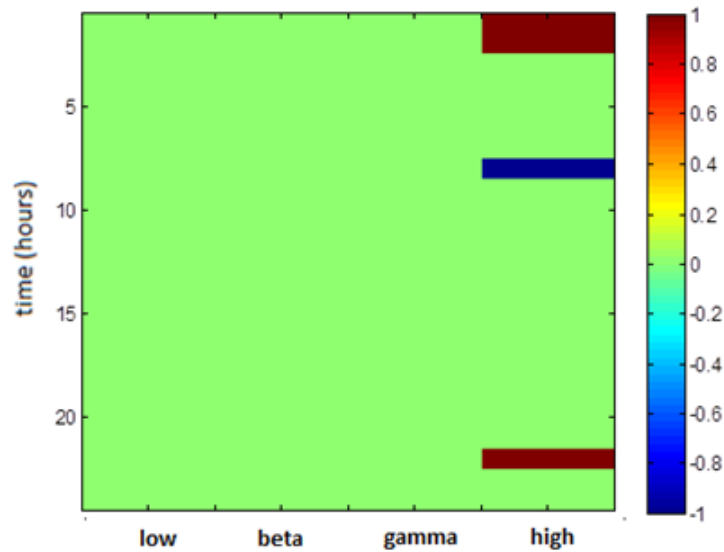


Figure 4-12. Same as Figure 4-11, but after injury.

Referring to rat #3, in Figures 4-13 and 4-14, the variations in relative power higher than 10% are shown, while in Figures 4-15 and 4-16, variations higher than 25% are considered.

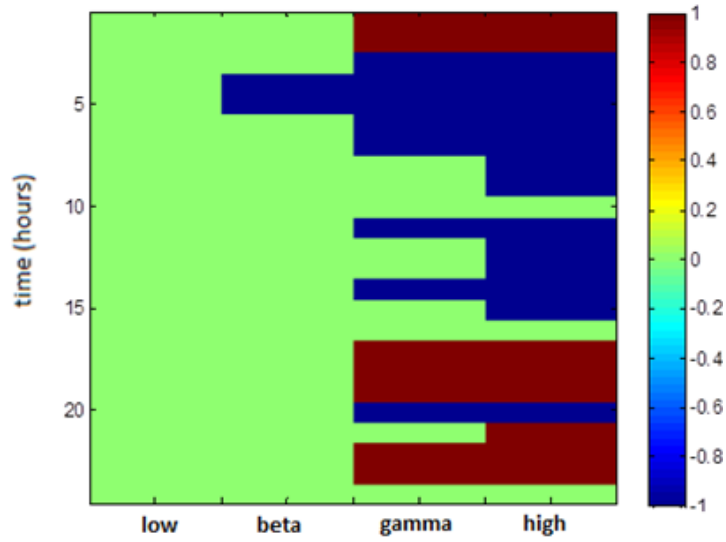


Figure 4-13. Distribution during the day of the variations in the relative power pre-injury. In red increases of more than 10%, in blue decreases. On the y-axis is the time of day, expressed so that 1 corresponds to 1 am and 24 to midnight.

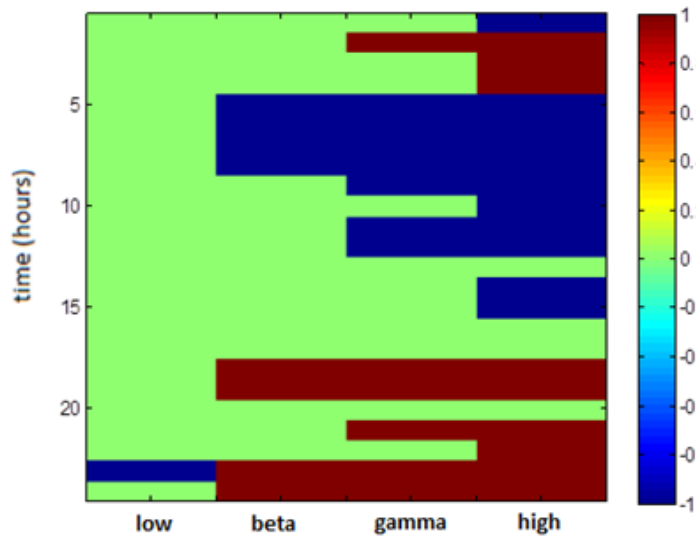


Figure 4-14. Same as Figure 4-13, but after injury

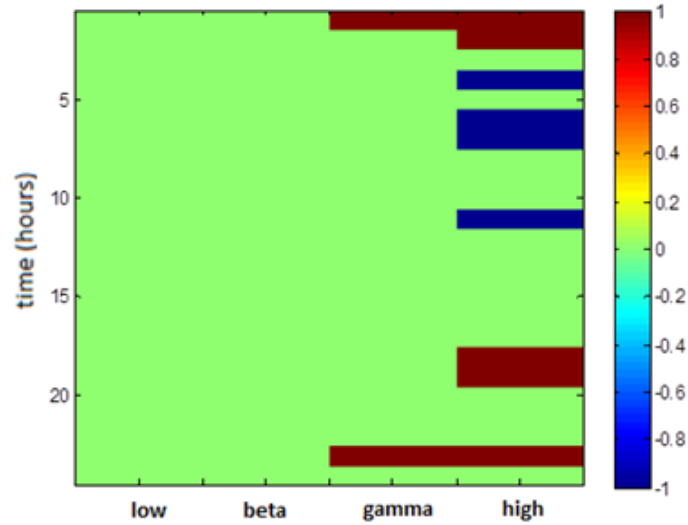


Figure 4-15. Distribution during the day of the variations in the relative power pre-injury. In red increases of more than 25%, in blue decreases. On the y-axis is the time of day, expressed so that 1 corresponds to 1 am and 24 to midnight.

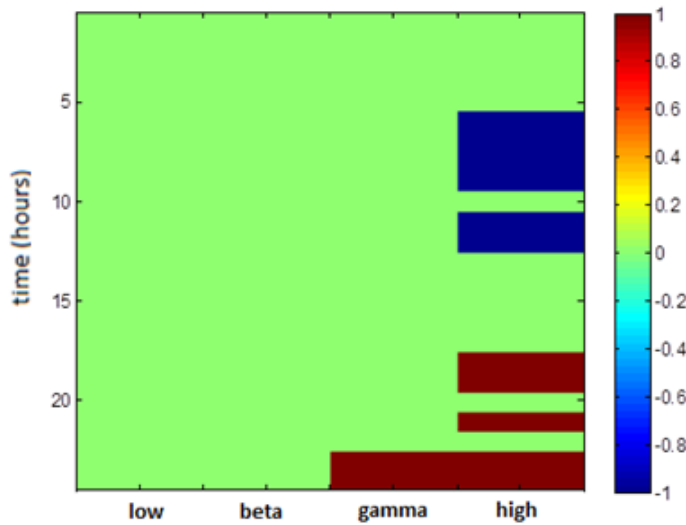


Figure 4-16. Same as Figure 4-15, but after injury.

In all the circumstances it can be observed that the daily variations in relative power follow the same pattern that is increases during the evening/night and decreases during the day. A summary of the results is given in Tables 4,5,6,7,8 and 9 and in Figures 4-17 and 4-18.

Table 4-4. Number of daily variations higher than 10% for all the bands of all the rats and average values, pre-injury

Pre				
	Rat #1	Rat #2	Rat #3	Avg pre
Low	0	0	0	0.00
Beta	3	2	2	2.33
Gamma	15	9	15	13.00
High	15	7	21	14.33
Total	33	18	38	29.67

Table 4-5. Number of daily variations higher than 10% for all the bands of all the rats and average values, post-injury

Post				
	Rat #1	Rat #2	Rat #3	Avg post
Low	0	0	1	0.33
Beta	15	4	8	9.00
Gamma	15	12	13	13.33
High	14	18	20	17.33
Total	44	34	42	40.00

Table 4-6. Difference in the daily variations higher than 10% for all the bands of all the rats and average values

Post-Pre				
	Rat #1	Rat #2	Rat #3	Avg post
Low	0	0	1	0.33
Beta	12	2	6	6.67
Gamma	0	3	-2	0.33
High	-1	11	-1	3.00
Total	11	16	4	10.33

Table 4-7. Number of daily variations higher than 25% for all the bands of all the rats and average values, pre-injury

Pre				
	Rat #1	Rat #2	Rat #3	Avg pre
Low	0	0	0	0.00
Beta	0	0	0	0.00
Gamma	2	2	2	2.00
High	1	1	9	3.67
Total	3	3	11	5.67

Table 4-8. Number of daily variations higher than 25% for all the bands of all the rats and average values, post-injury

Post	Rat #1	Rat #2	Rat #3	Avg post
Low	0	0	0	0.00
Beta	1	0	0	0.33
Gamma	7	0	2	3.00
High	5	4	11	6.67
Total	13	4	13	10.00

Table 4-9. Difference in the daily variations higher than 25% for all the bands of all the rats and average values

Post-Pre	Rat #1	Rat #2	Rat #3	Avg post
Low	0	0	0	0.00
Beta	1	0	0	0.33
Gamma	5	-2	0	1.00
High	4	3	2	3.00
Total	10	1	2	4.33

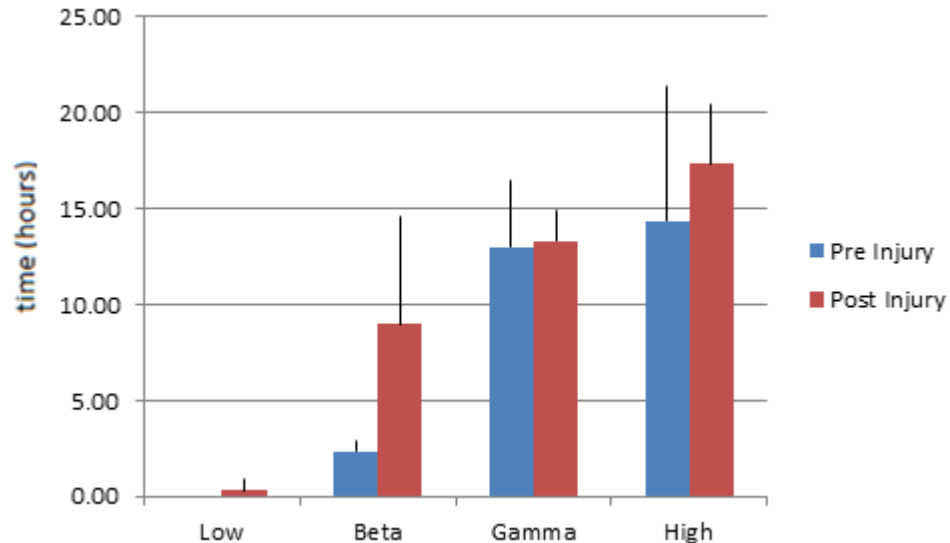


Figure 4-17. Column graph representing the number of variations >10% for each band pre injury and post injury. The error bars are expressed in terms of standard deviation.

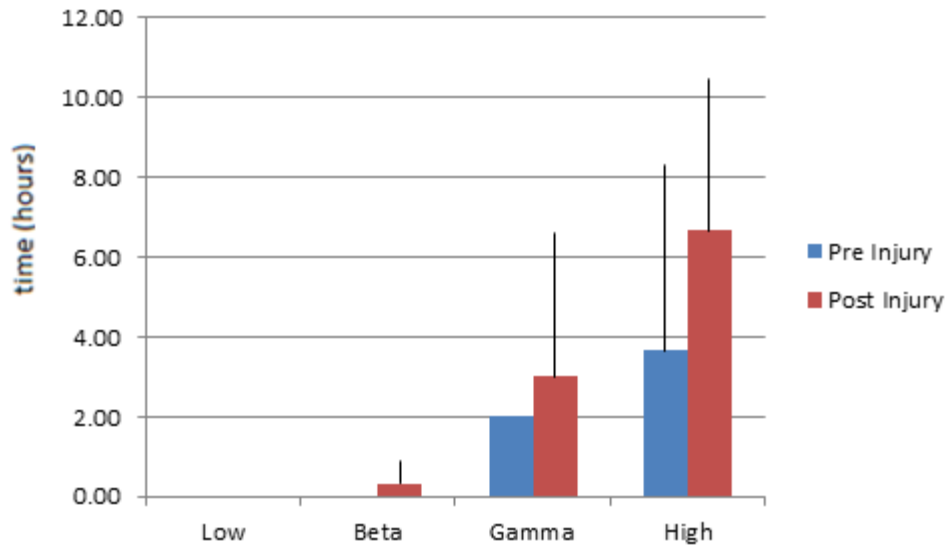


Figure 4-18. Column graph representing the number of variations >25% for each band pre injury and post injury. The error bars are expressed in terms of standard deviation.

Applying a paired t-test, it appeared that the increase in the number of variations higher than 10% for the beta band is statistically significant $p < 0.1$.

An increase in the number of variations in the beta band is consistent with the phase-shift observed, since the behavior of such band appears to become more similar to the one of the gamma and high bands, which have a higher number of such variations pre-injury than beta.

Considering variations higher than 25%, no statistically relevant difference is observed.

Relative Variations in Relative Power

In this paragraph the relative variations in relative power in the chronic phase with respect to the pre-injury phase are presented.

The results below refer to rat #1. Variations higher than 10% are shown in Figure 4-19, while variations higher than 25% are shown in Figure 4-20.

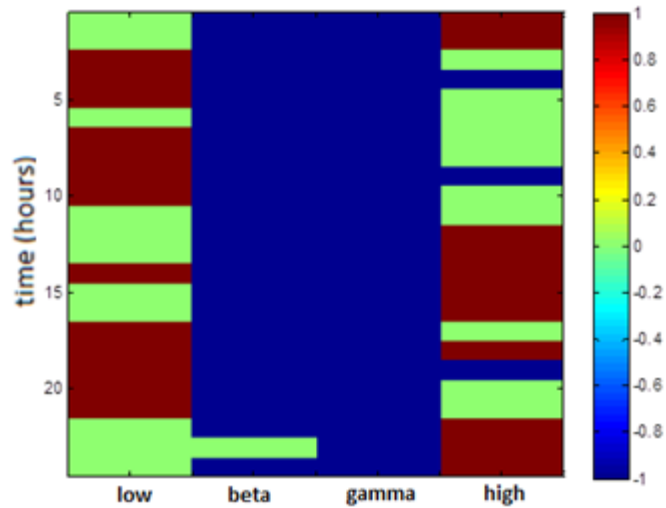


Figure 4-19. Distribution of the variations higher than 10%; in red increases, in blue decreases. On the y-axis is the time of day, expressed so that 1 corresponds to 1 am and 24 to midnight.

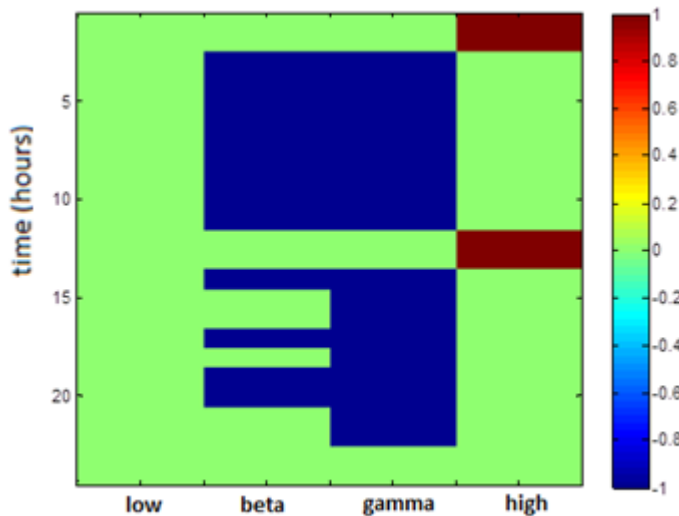


Figure 4-20. Distribution of the variations higher than 25%; in red increases, in blue decreases. On the y-axis is the time of day, expressed so that 1 corresponds to 1 am and 24 to midnight.

A consistent decrease in the beta and gamma bands can be observed. Some less relevant increases are seen in the low and high bands.

The results referring to rat #2 are presented below; in Figure 4-21 variations higher than 10%, in Figure 4-22 variations higher than 25%.

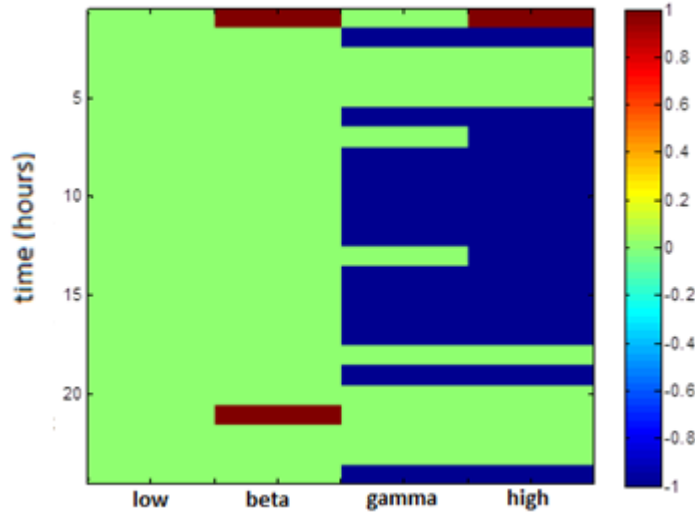


Figure 4-21. Distribution of the variations higher than 10%; in red increases, in blue decreases. On the y-axis is the time of day, expressed so that 1 corresponds to 1 am and 24 to midnight.

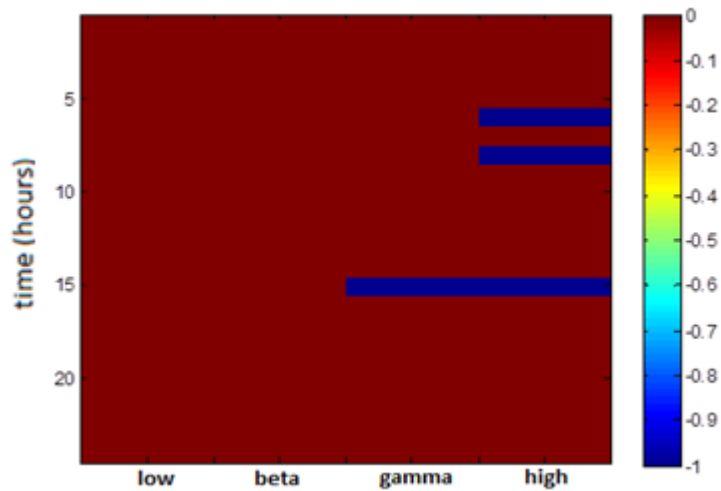


Figure 4-22. Distribution of the variations higher than 25%; in blue decreases. On the y-axis is the time of day, expressed so that 1 corresponds to 1 am and 24 to midnight.

Some decreases in the gamma and high bands can be observed, but only few of them are higher than 25%. The results referring to rat #3 are presented below; in Figure 4-23 variations higher than 10%, in Figure 4-24 variations higher than 25%.

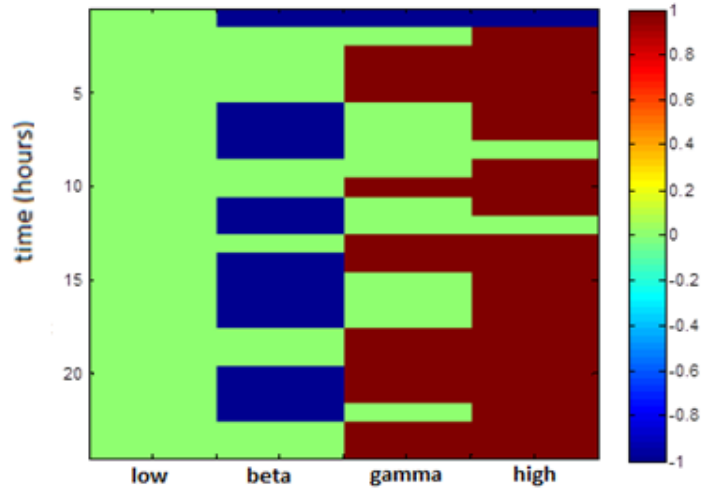


Figure 4-23. Distribution of the variations higher than 10%; in red increases, in blue decreases. On the y-axis is the time of day, expressed so that 1 corresponds to 1 am and 24 to midnight.

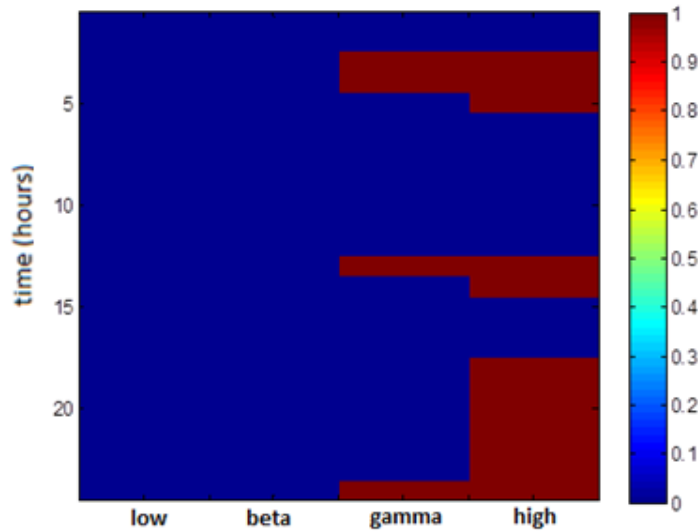


Figure 4-24. Distribution of the variations higher than 25%; in red increases. On the y-axis is the time of day, expressed so that 1 corresponds to 1 am and 24 to midnight.

In this case decreases in the beta and increases in the gamma and high can be observed. A summary of the results is given in Tables 10,11,12 and 13.

Table 4-10. Number of variations higher than 10% for all the bands for all the rats and average; (+) increases, (-) decreases

	Rat #1	Rat #2	Rat #3	Avg
Low	13(+)	0	0	4.33
Beta	23(-)	2(+)	13(-)	12.67
Gamma	24(-)	13(-)	13(+)	16.67
High	14(+)	16(-)	22(+)	17.33
Total	74	31	48	51.00

Table 4-11. Distribution pattern of the variations presented in Table 10; (+) increases, (-) decreases, D – during the day, N - during the night, (T) – throughout

	Rat #1	Rat #2	Rat #3	Majority
Low	DN (+T)	-	-	-
Beta	DN (-T)	N(+)	DN (-T)	DN (-T)
Gamma	DN (-T)	D(-)	DN (+T)	D(-)
High	DN(+)	D(-)	DN (+T)	DN(+)

Table 4-12. Number of variations higher than 25% for all the bands for all the rats and average; (+) increases, (-) decreases,

	Rat #1	Rat #2	Rat #3	Avg
Low	0	0	0	0.00
Beta	13(-)	0	0	4.33
Gamma	18(-)	1(-)	4(+)	7.67
High	4(+)	3(-)	12(+)	6.33
Total	35	4	16	18.33

Table 4-13. Distribution pattern of the variations presented in Table 12; in red increases, in blue decreases, D – during the day, N - during the night, (T) – throughout, (S) - sparse

	Rat #1	Rat #2	Rat #3	Majority
Low	-	-	-	-
Beta	DN (-T)	-	-	-
Gamma	DN (-T)	D(-)	DN (+S)	D(-)
High	DN(+)	D(-)	N(+)	N(+)

It can be seen that a clear pattern in this variations is lacking. This means that there isn't a specific mechanism or behavior emerging from the disease and the differences observed might be justified as the result of longer term modulation (supra-circadian rhythms) or other factors that weren't under direct control in this study.

Total Power

The daily variations in the total spectral power before and after injury are presented in this paragraph. The results referring to rats #1, #2 and #3 are given in Figures 4-25, 4-26 and 4-27 respectively.

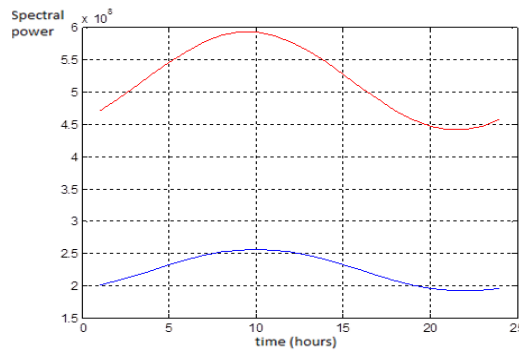


Figure 4-25. Circadian modulation of the total power for rat #1; in red pre-injury, in blue post-injury. On the x-axis is the time of day, expressed so that 1 corresponds to 1 am and 24 to midnight.

It can be observed that the total power still peaks at the same time.

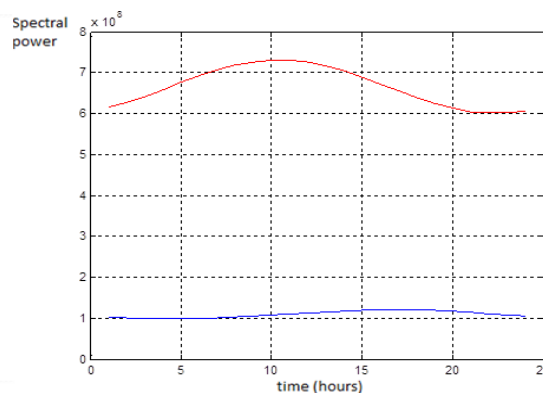


Figure 4-26. Circadian modulation of the total power for rat #2; in red pre-injury, in blue post-injury. On the x-axis is the time of day, expressed so that 1 corresponds to 1 am and 24 to midnight.

It can be observed that before injury the peak is at 10, while in the chronic phase it is around 16. It has to be said however that the sinusoid for the chronic phase has a relatively low amplitude and so, the accuracy in the estimation of the peak time is not extremely reliable.

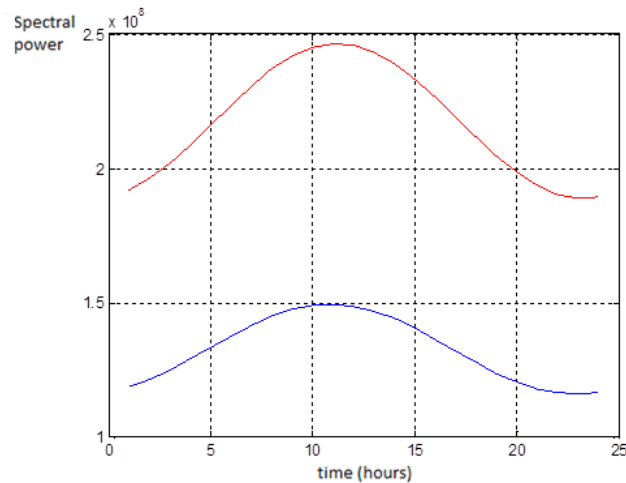


Figure 4-27. Circadian modulation of the total power for rat #3; in red pre-injury, in blue post-injury. On the x-axis is the time of day, expressed so that 1 corresponds to 1 am and 24 to midnight.

It can be observed that the total spectral power peaks at 11 both before and after the injury.

A summary of the results is given in Tables 14 and 15 and in Figure 4-28.

Table 4-14. Peak times of the total spectral power for all the rats and average, pre-injury

	Rat #1	Rat #2	Rat #3	Avg pre
Total pow	10	10	11	10.33

Table 4-15. Peak times of the total spectral power for all the rats and average, post-injury

Post	Rat #1	Rat #2	Rat #3	Avg post
Total pow	10	16	11	12.33

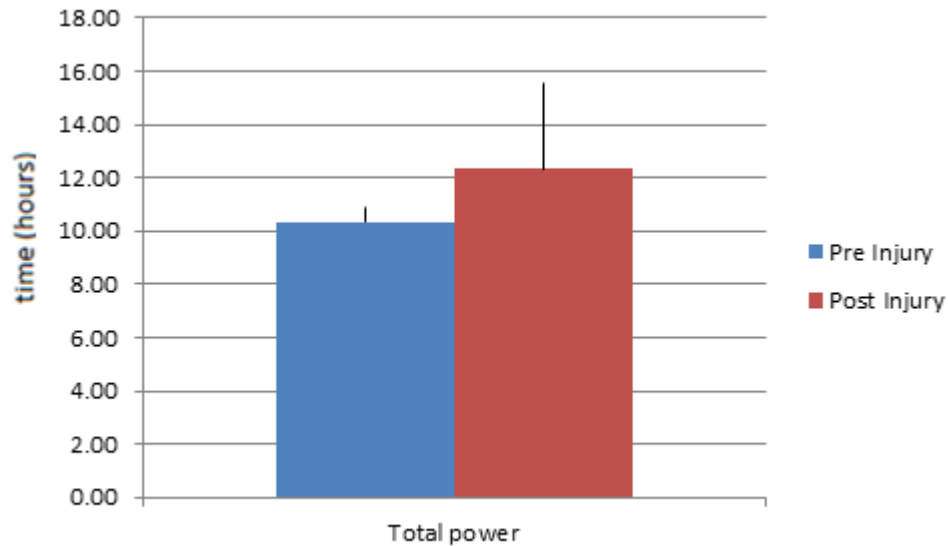


Figure 4-28. Column graph representing the peak time for the total power pre injury and post injury. On the y axis time of the day, where 1 is 1 am and 24 is midnight. The error bars are expressed in terms of standard deviation.

It can be said, after applying a paired t-test, that there is no statistically relevant difference in the peak time of the total spectral power before and after injury. This is consistent with the fact that the low band, where most of the spectral power is condensed, doesn't undergo a phase-shift.

CHAPTER 5 CONCLUSIONS

It clearly emerges from this study the fact that a phase-shift in the beta band occurs in the chronic phase of TLE during the interictal period. Furthermore, the phase-shift observed is in accordance to the one observed during the latent epileptogenic period [33], meaning that such a condition is not transient, but instead permanent. In [32] was shown that structural damage to the fimbria-fornix developed during the latency phase, as a result of the initial injury; it can be hypothesized that such structural damage causes the destruction of the path that allows the transmission of the circadian drive to the CA1 region, causing a disruption of the normal circadian modulation [31, 32, 33].

Since it has been proposed that beta rhythms might be used for high-level interactions between distant structures that can't be directly reached through gamma synchronization [13], it can be hypothesized that the phase-shift in the beta rhythms shown in this study might have some negative effects on cognition and memory. It is known, in fact, that jet lag causes a temporary reduction in intellectual performances [3] and the observed phase-shift might have the same effect, with the difference that this is sustained and not a transitory condition. TLE is frequently associated with cognitive and memory impairments, which are the result of a number of different factors such as the primary epileptogenic condition, the damaged caused by the seizures and the effects of the treatment [47, 48, 49, 50] and it can be thought that the observed phase-shift in the circadian modulation of beta rhythms might be one of the causes of the aforementioned cognitive impairments.

It has also been showed that seizures induce phase-shifts of rat circadian rhythms [51]. From this it can be hypothesized that seizures might act as a mechanism to reset the normal circadian modulation that has been disrupted by the brain injury; judging from [31, 32, 33], one might even hypothesize that the circadian modulation disruption is the driving factor leading to the development of TLE, at least in the cases that present hippocampal sclerosis, since epilepsy shows some symptoms similar to jet lag [52] and jet lag can induce seizures [53, 54]. It could be then be hypothesized that each seizure resets the normal circadian rhythms, but, due to the structural damage that prevent the circadian input to reach the CA1 region, the phase-shift observed will re-appear, leading to a new seizure and so on.

CHAPTER 6 FUTURE DEVELOPMENTS

This study led to a series of fascinating hypothesis, all of which would need further investigation in order to be tested. To start with, it would be interesting to prove if provoking the structural damage to the fimbria-fornix observed in [32] would lead to the same phase-shift in the beta rhythm observed in this study and/or seizures with characteristics comparable to the ones observed in TLE.

It would also be interesting to see if it is possible to induce seizures by forcing a sustained jet lag effect for several days or weeks (the temporal window of the latent epileptogenic phase). Finally it would be interesting to study the circadian dynamics between a series of spikes that occur at a distance of some days one to the other, in order to verify if the proposed hypothesis of the seizures as a reset mechanism for circadian modulation is consistent.

Last but not least, it would be of great interest to extend the results of this study to humans. This in order to verify if the observed phase-shift or other similar disruptions in circadian rhythms can be observed in human patients affected with TLE with hippocampal sclerosis.

LIST OF REFERENCES

- [1] J. Engel and T. A. Pedley, "Introduction: What Is Epilepsy?" in *Epilepsy: a Comprehensive Textbook*, vol. 1, Ed. Philadelphia: Lippincott-Raven, 1998, ch. 1, pp. 1-7.
- [2] M. N. Shouse and A. M. da Silva, "Chronobiology" in *Epilepsy: a Comprehensive Textbook*, vol. 2, J. Engel and T. A. Pedley, Ed. Philadelphia: Lippincott-Raven, 1998, ch. 181, pp. 1917-1928.
- [3] R. Refinetti, *Circadian Physiology*, Ed. Boca Raton: CRC Press, 2000.
- [4] P. Bailey, "The Purpose of Temporal Lobe Epilepsy – Purpose of Colloquium" in *Int. Colloq. Temporal Lobe Epilepsy*, Bethesda, MD, 1958, pp. 7-12.
- [5] D. Y. Ko, S. Sahai-Srivastava, S. R. Benbadis, J.E. Cavazos *et al.* (2012, Mar. 12), *Temporal Lobe Epilepsy* [Online]. Available: <http://emedicine.medscape.com/article/1184509-overview#a0101> .
- [6] S. Wiebe, "Epidemiology of Temporal Lobe Epilepsy", *Can. J. Neurol. Sci.*, vol. 1, no.1, pp. 6-10, May 2000.
- [7] G. L. Holmes (2006, Oct. 21), *Temporal Lobe Epilepsy* [Online]. Available: http://www.epilepsy.com/EPILEPSY/epilepsy_temporallobe .
- [8] G. W. Mathern, C. L. Wilson and H. Beck, "Hippocampal Sclerosis" in *Epilepsy: a Comprehensive Textbook*, vol. 1, Ed. Philadelphia: Lippincott-Raven, 1998, ch. 13, pp. 133-155.
- [9] H. Wieser, "Mesial Temporal Lobe Epilepsy with Hippocampal Sclerosis", *Epilepsia*, vol. 45, no. 6, pp. 695-714, May 2004.
- [10] H. M. Duvernoy, "Structure, Functions, and Connections", in *The Human Hippocampus: Functional Anatomy, Vascularization and Serial Sections with MRI*, Ed. New York: Springer, 2005, ch. 3, pp. 5-37.
- [11] R. B. Chronister and L. E. White, "Fiberarchitecture of the Hippocampal Formation: Anatomy, Projections, and Structural Significance", in *The Hippocampus*, vol.1, Ed. New York: Plenum Press, 1975, ch.1, pp. 9-39.
- [12] G. Buzsáki, "Generation of Hippocampal EEG Patterns", in *The Hippocampus*, vol. 3, Ed. New York: Plenum Press, 1975, ch. 5, pp. 137-167.
- [13] N. Kopell, G. B. Ermentrout, M. A. Whittington and R. D. Traub, "Gamma Rhythms and Beta Rhythms Have Different Synchronization Properties", *Proc. Nat. Academy Sci.*, vol. 97, no. 4, pp. 1867-1872, Feb. 2000.

- [14] J. O'Keefe, "Hippocampal Neurophysiology in the Behaving Animal", in *The Hippocampus Book*, Ed. New York: Oxford University Press, 2006, ch.11, pp. 475-548.
- [15] R. P. Vertes, "Brainstem Modulation of the Hippocampus: Anatomy, Physiology, and Significance", in *The Hippocampus*, vol. 4, Ed. New York: Plenum Press, 1975, ch. 2, pp. 41-75.
- [16] C. Pavlides, "Long-Term Potentiation in the Dentate Gyrus Is Induced Preferentially on the Positive Phase of Theta Rhythm", *Brain Res.*, vol. 439, no. 1-2, pp. 383-387, Jan. 1988.
- [17] M. V. Tsodyks, W. E. Skaggs, T. J. Sejnowski and B. L. McNaughton, "Population Dynamics and Theta Rhythm Phase Precession of Hippocampal Place Cell Firing: A Spiking Neuron Model", *Hippocampus*, vol. 6, no. 3, pp. 271-280, Mar. 1996.
- [18] G. Buzsáki, "Theta Rhythm of Navigation: Link Between Path Integration and Landmark Navigation, Episodic and Semantic Memory", *Hippocampus*, vol. 15, no. 7, pp. 827-840, Sep. 2005.
- [19] R. P. Vertes, W. B. Hoover and G. V. Di Prisco, "Theta Rhythm of the Hippocampus: Subcortical Control and Functional Significance", *Behav. Cogn. Neurosci. Rev.*, vol. 3, no. 3, pp. 173-200, Sep. 2004.
- [20] J. O'Keefe and M. L. Recce, "Phase Relationship Between Hippocampal Place Units and the EEG Theta Rhythm", *Hippocampus*, vol. 3, no. 3, pp. 317-330, Jul. 1993.
- [21] R. D. Traub, J. G. R. Jefferys and M. A. Whittington, "Conclusions: Are Gamma Oscillation Significant for Brain Function?", in *Fast Oscillations in Cortical Circuits*, Ed. Cambridge, Mass: MIT Press, 1999, ch. 11, pp. 267-272.
- [22] K. Longden, "Constraining the Function of CA1 in Associative Memory Models of the Hippocampus", Ph.D. dissertation, Sch. Informatics, Univ. Edinburgh, Edinburgh, UK, 2005.
- [23] M. Megías, Z. Emri, T. F. Freund and A. Gulyás, "Total Number and Distribution of Inhibitory and Excitatory Synapses on Hippocampal CA1 Pyramidal Cells", *Neurosci.*, vol. 102, no. 3, pp. 527-540, Feb. 2001.
- [24] N. Spruston and C. McBain, "Structural and Functional Properties of Hippocampal Neurons", in *The Hippocampus Book*, Ed. New York: Oxford University Press, 2006, ch. 5, pp. 133-201.
- [25] A. Treves and E. T. Rolls, "Computational analysis of the role of the hippocampus in memory", *Hippocampus*, vol. 4, no. 3, pp. 374-391, Jun. 1994.

- [26] J. L. McClellan and N. H. Goddard, "Considerations Arising From a Complementary Learning Systems Perspective on Hippocampus and Neocortex", *Hippocampus*, vol. 6, no. 6, pp. 654-665, Sep. 1996.
- [27] J. E. Lisman and N. A. Otmakhova, "Storage, Recall, and Novelty Detection of Sequences by the Hippocampus: Elaborating on the SOCRATIC Model to Account for Normal and Aberrant Effects of Dopamine", *Hippocampus*, vol. 11, no. 5, pp. 551-568, Oct. 2001.
- [28] M. E. Hasselmo, "The Role of Hippocampal Regions CA3 and CA1 in Matching Entorhinal Input With Retrieval of Associations Between Objects and Context: Theoretical Comment on Lee et al. (2005)", *Behav. Neurosci.*, vol. 119, no. 1, pp. 342-345, Feb. 2005.
- [29] X. Wu, J. Tyrcha and W. B. Levy, "A neural network solution to the transverse patterning problem depends on repetition of the input code", *Biol. Cybern.*, vol. 79, no. 3, pp. 203-213, Oct. 1998.
- [30] K. Longden and D. Willshaw, "An Evaluation of Recurrent Feedforward Memory Networks and their Relevance to the Hippocampus", *Neurocomp.*, vol. 44-46, pp. 527-531, Jun. 2002.
- [31] S. S. Talathi, D. U. Wang, W. L. Ditto, T. Mareci *et al.*, "Circadian control of neural excitability in an animal model of temporal lobe epilepsy", *Neurosci. Letters*, vol. 455, no. 2, pp. 145-149, May 2009.
- [32] D. A. Stanley, P. R. Carney, M. B. Parekh, T. Mareci *et al.*, "Phase Shift in Hippocampal Circadian Rhythm During the Latent Period of Epileptic Rats", *20th Annu. Computational Neuroscience Meeting*, Stockholm, Sweden, 2011, pp. 76.
- [33] D. A. Stanley, S. S. Talathi, X. Ni, L. Huang *et al.*, "Circadian Rhythms of Gamma Oscillations Following Status Epilepticus: Implications for Cognition", unpublished.
- [34] J. C. Sanchez, T. Mareci, W. M. Norman, J. C. Principe *et al.*, "Evolving into Epilepsy: Multiscale Electrophysiological Analysis and Imaging in an Animal Model", *Exp. Neurol.*, vol. 198, no. 1, pp. 31-47, Mar. 2006.
- [35] E. W. Lothman, E. H. Bertram, J. Kapur and J. L. Stringer, "Recurrent Spontaneous Hippocampal Seizures in the Rat as a Chronic Sequela to Limbic Status Epilepticus", *Epilepsy Res.*, vol. 6, no. 2, pp. 110-118, Jul. 1990.
- [36] E. H. Bertram and J. F. Cornett, "The Evolution of a Rat Model of Chronic Spontaneous Limbic Seizures", *Brain Res.*, vol. 661, no. 1-2, pp. 157-162, Oct. 1994.

- [37] E. W. Lothman, E. H. Bertram, J. W. Bekenstein and J. B. Perlin, "Self-Sustaining Limbic Status Epilepticus Induced by 'Continuous' Hippocampal Stimulation: Electrographic and Behavioral Characteristics", *Epilepsy Res.*, vol. 3, no. 2, pp. 107-119, Mar. 1989.
- [38] K. R. Rao, D. N. Kim J. J. Hwang, *Fast Fourier Transform: Algorithms and Applications*, Ed. New York: Springer, 2010.
- [39] I. Kaplan (2001, Oct.), *DFT of a Non-Stationary Time Series* [Online]. Available: http://www.bearcave.com/misl/misl_tech/signal/nonstat/index.html .
- [40] K. Lehnertz, "Non-Linear Time Series Analysis of Intracranial EEG Recordings in Patients with Epilepsy — An Overview", *Int. J. Psychophysiology*, vol. 34, no. 1, pp. 45-52, Oct. 1999.
- [41] J. Pardey, S. Roberts and L. Tarassenko, "A Review of Parametric Modelling Techniques for EEG Analysis", *Med. Eng. & Physics*, vol. 18, no. 1, pp. 2-11, Jan. 1996.
- [42] R. Acharya, O. Faust, N. Kannathal, T. Chua *et al.*, "Non-Linear Analysis of EEG Signals at Various Sleep Stages", *Comp. Methods & Programs Biomed.*, vol. 80, no. 1, pp. 37-45, Oct. 2005.
- [43] V. Navarro, J. Martinerie, M. Quyen, S. Clemencau *et al.*, "Seizure Anticipation in Human Neocortical Partial Epilepsy", *Brain*, vol. 125, no. 3, pp. 640-655, Feb. 2002.
- [44] A. Y. Kaplan and S. L. Shishkin, "Application of the Change-Point Analysis to the Investigation of the Brain's Electrical Activity", in *Nonparametric Statistical Diagnosis: Problems and Methods*, Ed: Dordrecht, The Netherlands: Kluwer Academic Publishers, 2000, ch. 7, pp. 333-388.
- [45] J. O. Smith (2011, Dec.), Spectral Audio Signal Processing [Online]. Available: <http://ccrma.stanford.edu/~jos/sasp/> .
- [46] J. B. Allen, "Short Term Spectral Analysis, Synthesis, and Modification by Discrete Fourier Transform", *IEEE Trans. Acoust., Speech, Signal Process.*, vol. 25, no. 3, pp. 235-238, Jun. 1977.
- [47] R. Mayeux, J. Brandt, J. Rosen and D. F. Benson, "Interictal Memory and Language Impairment in Temporal Lobe Epilepsy", *Neurology*, vol. 30, no. 2, pp. 120-125, Feb. 1980.
- [48] C. Helmstaedter and E. Kockelmann, "Cognitive Outcomes in Patients with Chronic Temporal Lobe Epilepsy", *Epilepsia*, vol. 47, no. 2, pp. 96-98, Nov. 2006.

- [49] C. Helmstaedter, M. Kurthen, S. Lux, M. Reuber *et al.*, "Chronic Epilepsy and Cognition: A Longitudinal Study in Temporal Lobe Epilepsy", *Ann. Neurol.*, vol. 54, no. 4, pp. 425-432, Oct. 2003.
- [50] H. Jokeit and A. Ebner, "Long Term Effects of Refractory Temporal Lobe Epilepsy on Cognitive Abilities: A Cross Sectional Study", *J Neurol Neurosurg Psychiatry*, vol. 67, no. 1, pp. 44-50, Jul. 1999.
- [51] M. Quigg, M. Straume, T. Smith, M. Menaker *et al.*, "Seizures Induce Phase Shifts of Rat Circadian Rhythms", *Brain Res.*, vol. 913, no. 2, pp. 165-169, Sep. 2001.
- [52] C. W. Bazil, D. Short, D Crispin and W. Zheng, "Patients with Intractable Epilepsy Have Low Melatonin, which Increases Following Seizures", *Neurology*, vol. 55, no. 11, pp. 1746-1748, Dec. 2000.
- [53] H Sei, H. Fujihara, Y. Ueta, K. Morita *et al.*, "Single Eight-Hour Shift of Light-Dark Cycle Increases Brain-Derived Neurotrophic Factor Protein Levels in the Rat Hippocampus", *Life Sci.*, vol. 73, no. 1, pp. 53-59, Mar. 2003.
- [54] T. Trevorrow, "Air Travel and Seizure Frequency for Individuals with Epilepsy", *Seizure*, vol. 15., no. 5, pp. 320-327, Jul. 2006.